Continuous kinematic wave models of merging traffic flow

Wen-Long Jin [*]

February 12, 2010

Abstract

Merging junctions are important network bottlenecks, and a better understanding of merging traffic dynamics has both theoretical and practical implications. In this paper, we present continuous kinematic wave models of merging traffic flow which are consistent with discrete Cell Transmission Models with various distribution schemes. In particular, we develop a systematic approach to constructing kinematic wave solutions to the Riemann problem of merging traffic flow in supply-demand space. In the new framework, Riemann solutions on a link consist of an interior state and a stationary state, subject to admissible conditions such that there are no positive and negative kinematic waves on the upstream and downstream links respectively. In addition, various distribution schemes in Cell Transmission Models are considered entropy conditions. In the proposed analytical framework, we prove that the stationary states and boundary fluxes exist and are unique for the Riemann problem for both fair and constant distribution schemes. We also discuss two types of invariant merge models, in which local

_____

[*]Department of Civil and Environmental Engineering, California Institute for Telecommunications and Information Technology, Institute of Transportation Studies, 4000 Anteater Instruction and Research Bldg, University of California, Irvine, CA 92697-3600. Tel: 949-824-1672. Fax: 949-824-8385. Email: wjin@uci.edu. Corresponding author

and discrete boundary fluxes are the same as global and continuous ones. With numerical examples, we demonstrate the validity of the analytical solutions of interior states, stationary states, and corresponding kinematic waves. Discussions and future studies are presented in the conclusion section.

Key words: Kinematic wave models; merging traffic; Riemann problems; Cell Transmission Models; distribution schemes; supply-demand space; stationary states; interior states; boundary fluxes; invariant merge models

1 Introduction

In a road network, bottlenecks around merging, diverging, and other network junctions can cause the formation, propagation, and dissipation of traffic queues. For example, upstream queues can form at a merging junction due to the limited capacity of the downstream branch; at a diverging junction, when a queue forms on one downstream branch, the flow to the other downstream branch will be reduced, since the upstream link will be blocked due to the First-In-First-Out principle on the upstream link (Papageorgiou, 1990). Theoretically, a better understanding of merging traffic flow will be helpful for analyzing and understanding traffic dynamics on a road network (Nie and Zhang, 2008; Jin, 2009). Practically, it will be helpful for designing metering schemes (Papageorgiou and Kotsialos, 2002) and for understanding dynamic user equilibrium and drivers' route choice behaviors (Peeta and Ziliaskopoulos, 2001).

In the literature, a number of microscopic models have been proposed for vehicles' merging behaviors (e.g. Hidas, 2002, 2005). Due to the complicated interactions among vehicles, microscopic models are not suitable for analyzing merging traffic dynamics at the network level. At the macroscopic level, many attempts have been made to model merging traffic flow in the line of the LWR model (Lighthill and Whitham, 1955; Richards, 1956), which describes traffic dynamics with kinematic waves, including shock and rarefaction waves, in density (ρ), speed (v), and flux

(q). Based on a continuous version of traffic conservation, $\frac{\partial \rho}{\partial t} + \frac{\partial q}{\partial x} = 0$, and an assumption of a speed-density relationship, $v = V(\rho)$, the LWR model can be written as

$$\frac{\partial}{\partial t}\rho + \frac{\partial}{\partial x}\rho V(\rho) = 0, \tag{1}$$

which is for a homogeneous road link with time and location independent traffic characteristics, such as free flow speed, jam density, capacity, and so on. In general, $V(\rho)$ is a non-increasing function, and $v_f = V(0)$ is the free flow speed. In addition, $q = Q(\rho) \equiv \rho V(\rho)$ is unimodal with capacity $C = Q(\rho_c)$, where ρ_c is the critical density. If we denote the jam density by ρ_j, then $\rho \in [0, \rho_j]$.

In one line, Daganzo (1995) and Lebacque (1996) extended the Godunov discrete form of the LWR model and developed a new framework, referred to as Cell Transmission Models (CTM) hereafter, for numerically computing traffic flows through merging, diverging, and general junctions. In this framework, local traffic demand (i.e., sending flow) and supply (i.e., receiving flow) functions are introduced, and boundary fluxes through various types of junctions can be written as functions of upstream demands and downstream supplies. In the CTM framework, various distribution schemes can be employed to uniquely determine merging flows from all upstream links (Daganzo, 1995; Lebacque, 1996; Jin and Zhang, 2003; Ni and Leonard, 2005). These discrete merge models are physically intuitive, and stationary distribution patterns of merging flows have been observed and calibrated for various merging junctions (Cassidy and Ahn, 2005; Bar-Gera and Ahn, 2009). Such merge models are discrete in nature and can be used to simulate macroscopic traffic dynamics efficiently. However, there have been no systematic approaches to analyzing kinematic waves arising at a merging junction with these models.

In the other line, Holden and Risebro (1995) and Coclite et al. (2005) attempted to solve a Riemann problem of a highway intersection with m upstream links and n downstream links. In both of these studies, all links are homogeneous and have the same speed-density relations, and traffic dynamics on each link are described by the LWR model. In (Holden and Risebro, 1995), the Rie-

3

mann problem is solved by introducing an entropy condition that maximizes an objective function in all boundary fluxes. In (Coclite et al., 2005), the Riemann problem is solved to maximize total flux with turning proportions. Both studies were able to describe kinematic waves arising from a network intersection but also subject to significant shortcomings: (i) All links are assumed to have the same fundamental diagram in both studies; (ii) In (Holden and Risebro, 1995), the entropy conditions are pragmatic and lack of physical interpretations; and (iii) In (Coclite et al., 2005), the Riemann problem can only be uniquely solved for junctions with no fewer downstream links, and hence their results do not apply to a merging junction.

In this paper, we are interested in studying continuous kinematic wave models of merging traffic flow which are consistent with discrete CTM with various distribution schemes. Here we consider a merge network with $m \geq 2$ upstream links and one downstream link, as shown in Figure 1. In this network, there are $m+1$ links, m origin-destination pairs, and m paths. In the continuous kinematic wave models of this network, traffic dynamics on each link are described by the LWR model (1), and, in addition, an entropy condition based on various distribution schemes is used to pick out unique physical solutions (Ansorge, 1990). Note that traffic dynamics on the whole network cannot be modeled by either one-dimensional or two-dimensional conservation laws in closed forms, since vehicles of different commodities interact with each other on the downstream link. Similar to the LWR model, it is not possible to obtain analytical solutions for general initial and boundary conditions, and we usually resort to analyzing continuous kinematic wave solutions to Riemann problems. Studies on the Riemann problem are helpful for understanding fundamental characteristics of the corresponding merge model and constructing numerical solutions. In the Riemann problem, all links are homogeneous and infinitely long; for link $a = 1, \cdots, m+1$, we assume that its flow-density relation is $q_a = Q_a(\rho_a)$, critical density $\rho_{c,a}$, and its capacity C_a; and upstream link $i = 1, \cdots, m$ and downstream link $m+1$ have constant initial conditions:

$$\rho_i(x_i, 0) \quad = \quad \rho_i, \, x_i \in (-\infty, 0), \quad i = 1, \cdots, m \tag{2}$$

4

$$\rho_{m+1}(x_{m+1}, 0) = \rho_{m+1}, x_{m+1} \in (0, +\infty). \tag{3}$$

To pick out physical kinematic wave solutions to the Riemann problem, here we use various distribution schemes of CTM as our entropy conditions, which are different from the optimization-based entropy condition in (Holden and Risebro, 1995). In this sense, the resulted models can be considered as continuous versions of CTM with various distribution schemes.
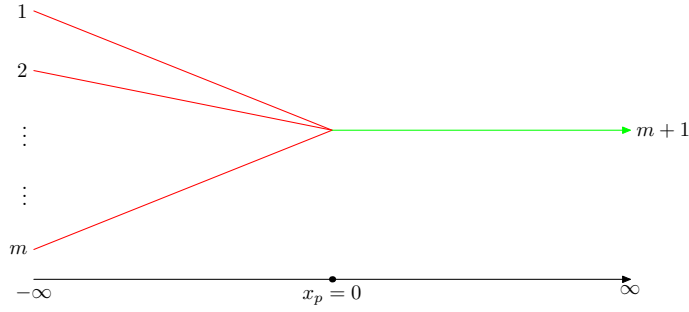

Figure 1: An illustration of a merge network

In our study, the upstream links can be mainline freeways or on-ramps with different characteristics, and our solutions are physically meaningful and consistent with discrete CTM of merging traffic. In addition, we follow a new framework developed in (Jin et al., 2009) for solving the Riemann problem for inhomogeneous LWR model at a linear junction. In this framework, we first construct Riemann solutions of a merge model in the supply-demand space: on each branch, a stationary state will prevail after a long time, and an interior state may exist but does not take any space in the continuous solution and only shows up in one cell in the numerical solutions (van Leer, 1984). After deriving admissible solutions for upstream and downstream stationary and interior states, we introduce an entropy condition consistent with various discrete merge models. We then prove that stationary states and boundary fluxes are unique for given upstream demands and downstream supply, and interior states may not be unique but inconsequential. Then, the kinematic wave on a link is uniquely determined by the corresponding LWR model with the stationary state and the initial state as initial states.

5

In this study, we do not attempt to develop new simulation models. Rather, we attempt to understand kinematic wave solutions of continuous merge models consistent with various CTM. The theoretical approach is not meant to replace numerical methods in CTM but to provide insights on the formation and dissipation of shock and rarefaction waves for the Riemann problem. In this study, we choose to solve the Riemann problem in supply-demand space due to its mathematical tractability. In fact, the benefits of working in the supply-demand space have been demonstrated by Daganzo (1995) and Lebacque (1996) when they developed discrete supply-demand models of network vehicular traffic, i.e., CTM. In their studies, the introduction of the concepts of demand and supply enabled a simple and intuitive formulation of merge and diverge models. But different from these studies, which focused on discrete simulation models, this study further introduces supply-demand diagram and discusses analytical solutions of continuous merge models.

The rest of the paper is organized as follows. In Section 2, we introduce an analytical framework for solving the kinematic waves of the Riemann problem with jump initial conditions in supply-demand space. In particular, we derive traffic conservation conditions, admissible conditions of stationary and initial states, and additional entropy conditions consistent with discrete merge models. In Section 3, we solve stationary states and boundary fluxes for both fair and constant merge models. In Section 4, we introduce two invariant merge models. In Section 5, we demonstrate the validity of the proposed analytical framework with numerical examples. In Section 6, we summarize our findings and present some discussions.

2   An analytical framework

For link $a = 1, \cdots, m+1$, we define the following demand and supply functions with all subscript a suppressed (Engquist and Osher, 1980; Daganzo, 1995; Lebacque, 1996)

$$D(\rho) \;=\; Q(\min\{\rho, \rho_c\}) = \begin{cases} Q(\rho), & \text{if } \rho \leq \rho_c \\ C, & \text{if } \rho \geq \rho_c \end{cases},$$

$$= \int_0^\rho \chi(s)Q'(s)ds = \int_0^\rho \max\{Q'(s),0\}ds \tag{4}$$

$$S(\rho) = Q(\max\{\rho,\rho_c\}) = \begin{cases} Q(\rho), & \text{if } \rho \geq \rho_c \\ C, & \text{if } \rho \leq \rho_c \end{cases},$$

$$= C + \int_0^\rho (1-\chi(s))Q'(s)ds = C + \int_0^\rho \min\{Q'(s),0\}ds, \tag{5}$$

where $\chi(\rho)$ equals 1 iff $Q'(\rho) \geq 0$ and equals 0 otherwise.

Unlike many existing studies, in which traffic states are considered in ρ-q space, we represent a traffic state in supply-demand space as $U = (D,S)$. For the demand and supply functions in (4) and (5), we can see that D is non-decreasing with ρ and S non-increasing. Thus $D \leq C$, $S \leq C$, $\max\{D,S\} = C$, and flow-rate $q(U) = \min\{D,S\}$. In addition, $D = S = C$ iff traffic is critical; $D < S = C$ iff traffic is strictly under-critical (SUC); $S < D = C$ iff traffic is strictly over-critical (SOC). Therefore, state $U = (D,S)$ is under-critical (UC), iff $S = C$, or equivalently $D \leq S$; State $U = (D,S)$ is over-critical (OC), iff $D = C$, or equivalently $S \leq D$.

In Figure 2(b), we draw a supply-demand diagram for the two fundamental diagrams in Figure 2(a). On the dashed branch of the supply-demand diagram, traffic is UC and $U = (D,C)$ with $D \leq C$; on the solid branch, traffic is OC and $U = (C,S)$ with $S \leq C$. Compared with the fundamental diagram of a road section, the supply-demand diagram only considers its capacity C and criticality, but not other detailed characteristics such as critical density, jam density, or the shape of the fundamental diagram. That is, different fundamental diagrams can have the same demand-supply diagram, as long as they have the same capacity and are unimodal. However, given a demand-supply diagram and its corresponding fundamental diagram, the points are one-to-one mapped.

In supply-demand space, initial conditions in (2) and (3) are equivalent to [1]

$$U_i(x_i,0) = (D_i,S_i), \quad x_i \in (-\infty,0), \tag{6}$$

$$U_{m+1}(x_{m+1},0) = (D_{m+1},S_{m+1}), \quad x_{m+1} \in (0,+\infty). \tag{7}$$

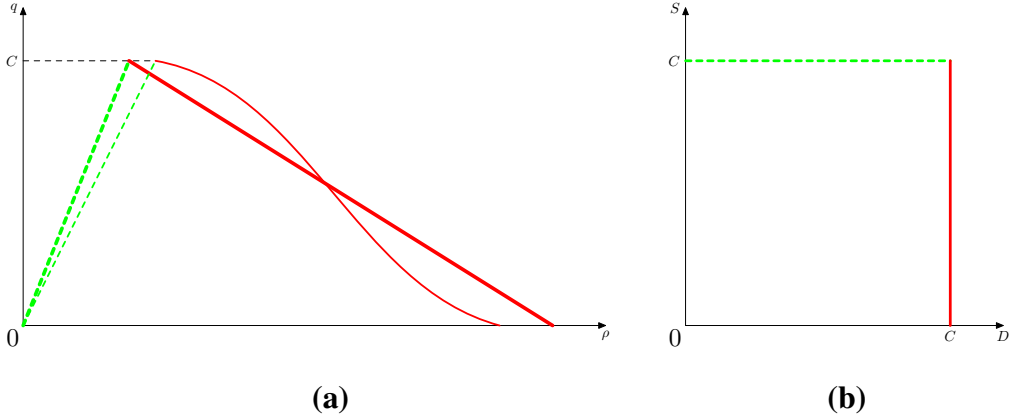[1] In this section, $i = 1, \cdots, m$ if not otherwise mentioned.

Figure 2: Fundamental diagrams and their corresponding supply-demand diagrams

In the solutions of the Riemann problem with initial conditions (6-7), a shock wave or a rarefaction wave could initiate on a link from the merging junction $x = 0$, and traffic states on all links become stationary after a long time. That is, in solutions to the Riemann problem, stationary states prevail all links after a long time. At the boundary, there can also exist interior states (van Leer, 1984; Bultelle et al., 1998), which take infinitesimal space [2]. We denote the stationary states on upstream link i and downstream link $m+1$ by U_i^- and U_{m+1}^+, respectively. We denote the interior states on links i and $m+1$ by $U_i(0^-,t)$ and $U_{m+1}(0^+,t)$, respectively. The structure of Riemann solutions on upstream and downstream links are shown in Figure 3, where arrows illustrate the directions of possible kinematic waves. Then the kinematic wave on upstream link i is the solution of the corresponding LWR model with initial left and right conditions of U_i and U_i^-, respectively. Similarly, the kinematic wave on downstream link $m+1$ is the solution of the corresponding LWR model with initial left and right conditions of U_{m+1}^+ and U_{m+1}, respectively.

We denote $q_{i \to m+1}$ as the flux from link i to link $m+1$ for $t > 0$. The fluxes are determined by the stationary states: the out-flux of link i is $q_i = q(U_i^-)$, and the in-flux of link $m+1$ is

_____

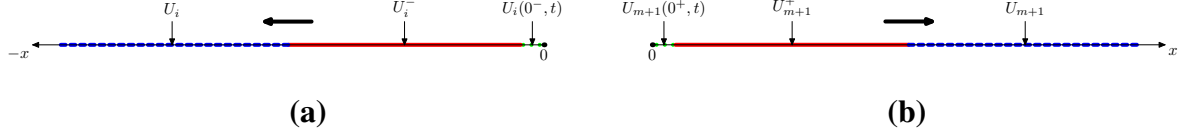[2]In numerical solutions, the interior states exist in one cell.

8

Figure 3: The structure of Riemann solutions: (a) Upstream link i; (b) Downstream link $m+1$

$q_{m+1} = q(U_{m+1}^+)$. Furthermore, from traffic conservation at a merging junction, we have

$$q_{i \to m+1} = q_i = q(U_i^-), \quad q_{m+1} = q(U_{m+1}^+) = \sum_{i=1}^{m} q(U_i^-). \qquad (8)$$

2.1 Admissible stationary and interior states

As observed in (Holden and Risebro, 1995; Coclite et al., 2005), the speed of a kinematic wave on an upstream link cannot be positive, and that on a downstream link cannot be negative. We have the following admissible conditions on stationary states.

Theorem 2.1 (Admissible stationary states) *For initial conditions in (6) and (7), stationary states are admissible if and only if*

$$U_i^- = (D_i, C_i) \ or \ (C_i, S_i^-), \qquad (9)$$

where $S_i^- < D_i$, and

$$U_{m+1}^+ = (C_{m+1}, S_{m+1}) \ or \ (D_{m+1}^+, C_{m+1}), \qquad (10)$$

where $D_{m+1}^+ < S_{m+1}$.

The proof is quite straightforward and omitted here. The regions of admissible upstream stationary states in both supply-demand and fundamental diagrams are shown in Figure 4, and the regions of admissible downstream stationary states are shown in Figure 5. In Figure 4(a) and (b), the initial upstream condition is SUC with $D_i < C_i = S_i$, and feasible stationary states are (D_i, C_i), when there is no wave, or (C_i, S_i^-) with $S_i^- < D_i$, when a back-traveling shock wave emerges on the

9

upstream link i; In Figure 4(c) and (d), the initial upstream condition is OC with $S_i \leq D_i = C_i$, and any OC stationary state is feasible, when a back-traveling shock or rarefaction wave emerges on the upstream link i. In contrast, in Figure 5(a) and (b), the initial downstream condition is UC with $D_{m+1} \leq S_{m+1} = C_{m+1}$, and any UC stationary state is feasible, when a forward-traveling shock or rarefaction wave emerges on the downstream link $m+1$; In Figure 5(c) and (d), the initial downstream condition is SOC with $S_{m+1} < D_{m+1} = C_{m+1}$, and feasible stationary states are (C_{m+1}, S_{m+1}), when there is no wave, or (D_{m+1}^+, C_{m+1}) with $D_{m+1}^+ < S_{m+1}$, when a forward-traveling shock wave emerges on the downstream link $m+1$. Here the types of kinematic waves and the signs of the wave speeds can be determined in the supply-demand diagram, but the absolute values of the wave speeds have to be determined in the fundamental diagram.
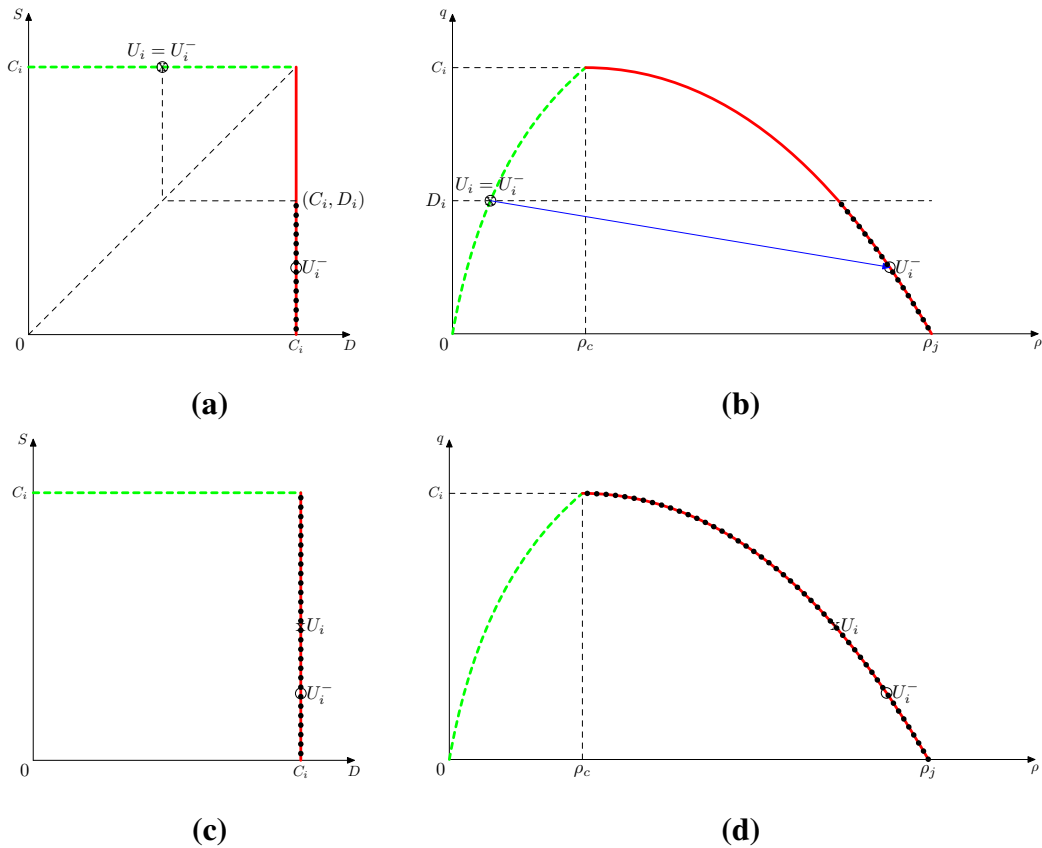

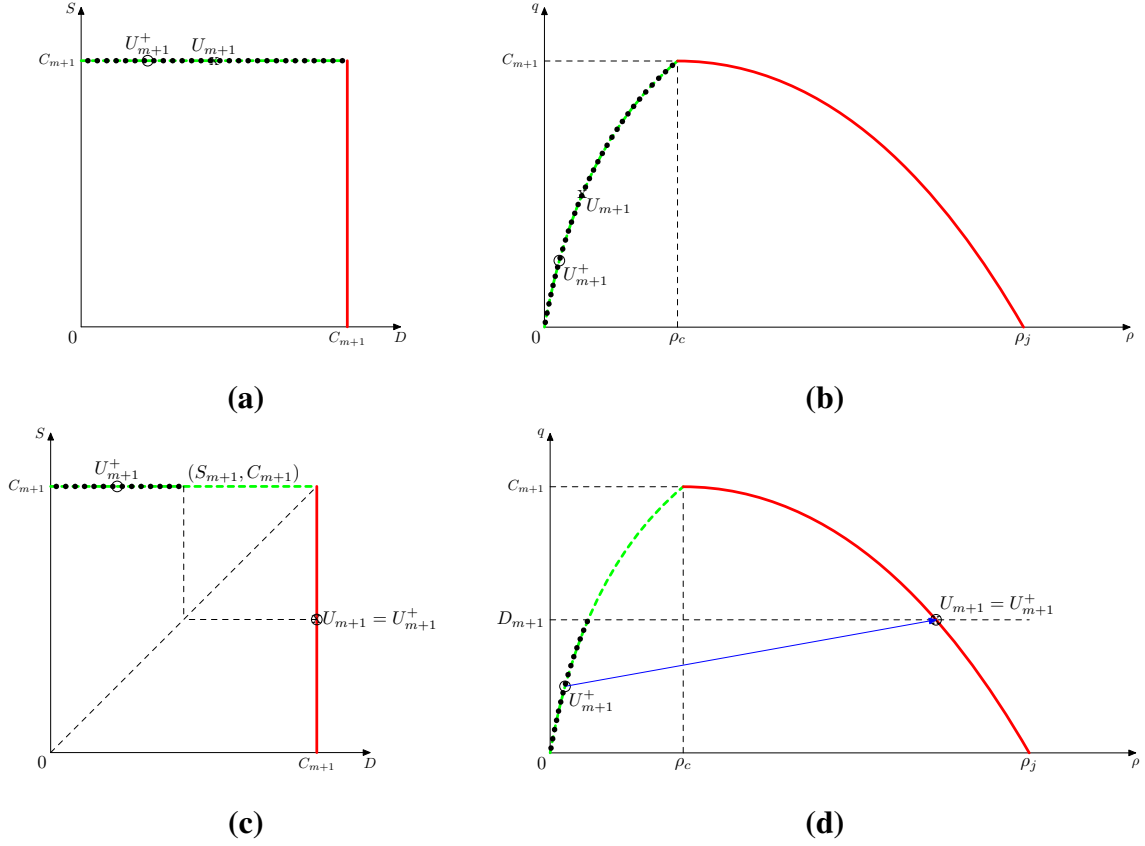Figure 4: Admissible stationary states for upstream link i: marked by black dots

Figure 5: Admissible stationary states for downstream link $m+1$: marked by black dots

Remark 1. $U_i^- = U_i$ and $U_{m+1}^+ = U_{m+1}$ are always admissible. In this case, the stationary states are the same as the corresponding initial states, and there are no waves.

Remark 2. Out-flux $q_i = \min\{D_i^-, S_i^-\} \leq D_i$ and in-flux $q_{m+1} = \min\{D_{m+1}^+, S_{m+1}^+\} \leq S_{m+1}$. That is, D_i is the maximum sending flow and S_{m+1} is the maximum receiving flow in the sense of (Daganzo, 1994, 1995).

Remark 3. The "invariance principle" in (Lebacque and Khoshyaran, 2005) can be interpreted as follows: if $D_i^- = C_i$, then $q(U_i^-) < D_i$; if $S_{m+1}^+ = C_{m+1}$, then $q(U_{m+1}^+) < S_i$. We can see that Theorem 2.1 is consistent with the "invariance principle".

Corollary 2.2 *For the upstream link i, $q_i \leq D_i$; $q_i < D_i$ if and only if $U_i^- = (C_i, q_i)$, and $q_i = D_i$*

if and only if $U_i^- = (D_i, C_i)$. For the downstream link $m+1$, $q_{m+1} \leq S_{m+1}$; $q_{m+1} < S_{m+1}$ if and only if $U_{m+1}^+ = (q_{m+1}, C_{m+1})$, and $q_{m+1} = S_{m+1}$ if and only if $U_{m+1}^+ = (C_{m+1}, S_{m+1})$. That is, given out-fluxes and in-fluxes, the stationary states can be uniquely determined.

For interior states, the waves of the Riemann problem on link i with left and right initial conditions of U_i^- and $U_i(0^-, t)$ cannot have negative speeds. Similarly, the waves of the Riemann problem on link $m+1$ with left and right initial conditions of $U_{m+1}(0^+, t)$ and U_{m+1}^+ cannot have positive speeds. Therefore, interior states $U_i(0^-, t)$ and $U_{m+1}(0^+, t)$ should satisfy the following admissible conditions.

Theorem 2.3 (Admissible interior states) *For stationary states U_i^- and U_{m+1}^+, interior states $U_i(0^-, t)$ and $U_{m+1}(0^+, t)$ are admissible if and only if*

$$U_i(0^-, t) = \begin{cases} (C_i, S_i^-) = U_i^-, & \text{when } U_i^- \text{ is SOC; i.e., } S_i^- < D_i^- = C_i \\ (D_i(0^-, t), S_i(0^-, t)), & \text{when } U_i^- \text{ is UC; i.e., } D_i^- \leq S_i^- = C_i \end{cases} \quad (11)$$

where $S_i(0^-, t) \geq D_i^-$, and

$$U_{m+1}(0^+, t) = \begin{cases} (D_{m+1}^+, C_{m+1}) = U_{m+1}^+, & \text{when } U_{m+1}^+ \text{ is SUC; i.e., } D_{m+1}^+ < S_{m+1}^+ = C_{m+1} \\ (D_{m+1}(0^+, t), S_{m+1}(0^+, t)), & \text{when } U_{m+1}^+ \text{ is OC; i.e., } S_{m+1}^+ \leq D_{m+1}^+ = C_{m+1} \end{cases} \quad (12)$$

where $D_{m+1}(0^+, t) \geq S_{m+1}^+$.

The proof is quite straightforward and omitted here. The regions of admissible upstream interior states in both supply-demand and fundamental diagrams are shown in (6), and the regions of admissible downstream interior states are shown in (7). From the figures, we can also determine the types and traveling directions of waves with given stationary and interior states on all links, but these waves are suppressed and cannot be observed. Note that, however, we are able to observe possible interior states in numerical solutions.

Remark 1. Note that $U_i(0^-, t) = U_i^-$ and $U_{m+1}(0^+, t) = U_{m+1}^+$ are always admissible. In this case, the interior states are the same as the stationary states.
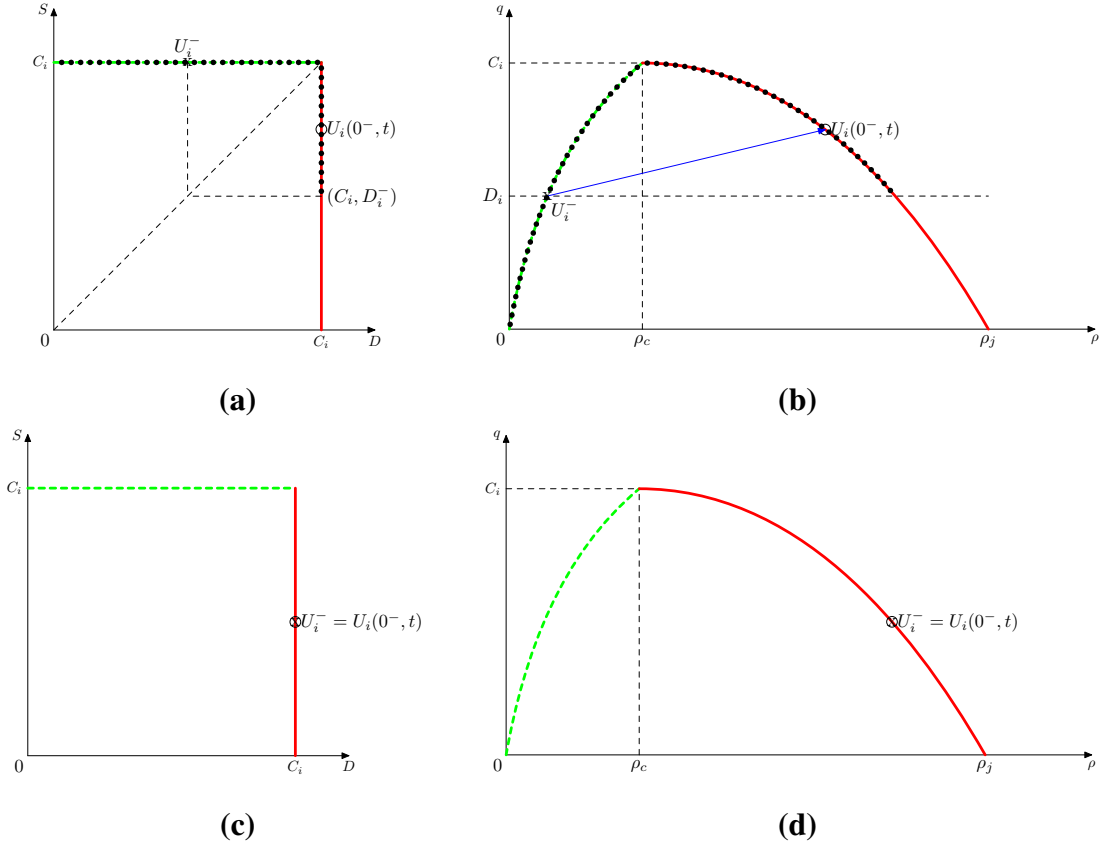
12

(a)

(b)

(c)

(d)

Figure 6: Admissible interior states for upstream link i: marked by black dots

2.2 Entropy conditions consistent with discrete merge models

In order to uniquely determine the solutions of stationary states, we introduce a so-called entropy condition in interior states as follows:

$$q_i \;=\; F_i(U_1(0^-,t),\cdots,U_m(0^-,t),U_{m+1}(0^+,t)). \tag{13}$$

The entropy condition can also be written as

$$q_{m+1} \;=\; F(U_1(0^-,t),\cdots,U_m(0^-,t),U_{m+1}(0^+,t)),$$
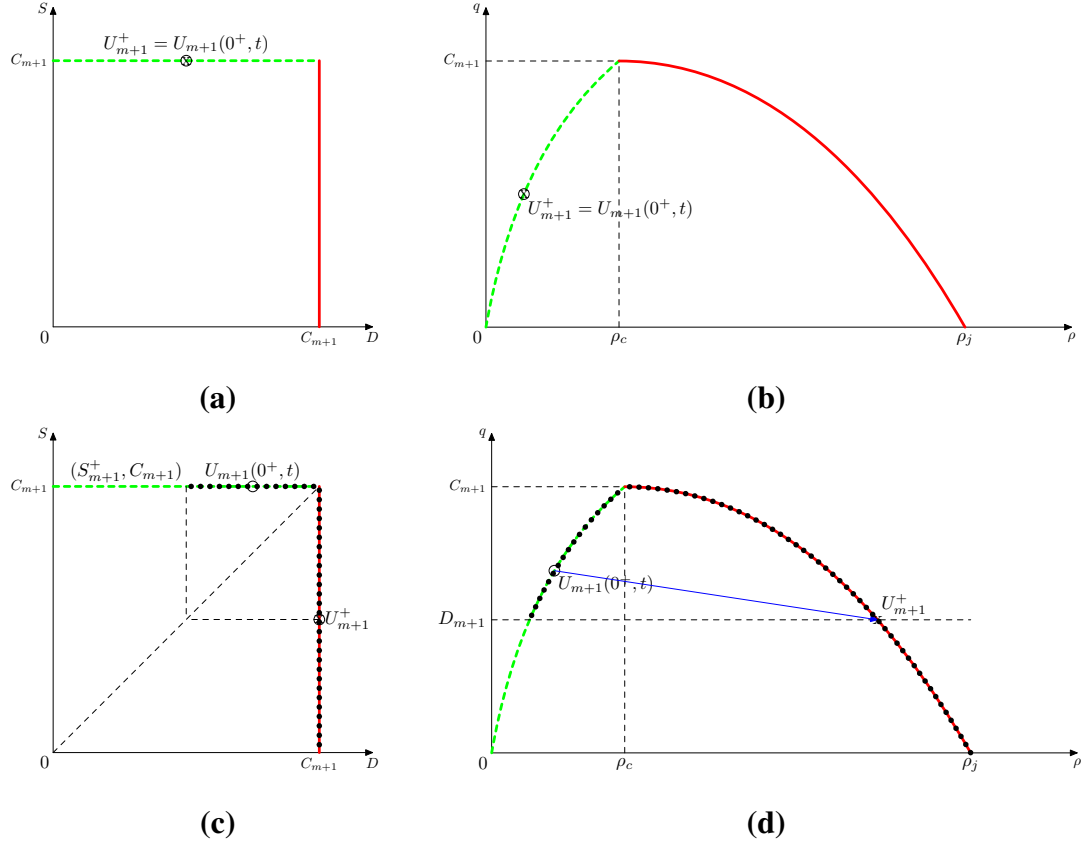$$q_i \;=\; \alpha_i q_{m+1},$$

13

Figure 7: Admissible interior states for downstream link $m+1$: marked by black dots

where $\alpha_i \in [0,1]$ and $\sum_{i=1}^{m} \alpha_i = 1$. We can see that the entropy condition uses "local" information in the sense that it determines boundary fluxes from interior states. In the discrete merge model, the entropy condition is used to determine boundary fluxes from cells contingent to the merging junction. Thus, $F_i(U_1(0^-,t),\cdots,U_m(0^-,t),U_{m+1}(0^+,t))$ in (13) can be considered as local, discrete flux functions.

Here the boundary fluxes can be obtained with existing merge models. In (Daganzo, 1995), $F(U_1(0^-,t),\cdots,U_m(0^-,t),U_{m+1}(0^+,t))$ was proposed to solve the following local optimization problem

$$\max_{U_i^-,U_{m+1}^+,U_i(0^-,t),U_{m+1}(0^+,t)} \{q_{m+1}\} \tag{14}$$

14

subject to

$$q_i \leq D_i(0^-,t),$$

$$q_{m+1} \leq S_{m+1}(0^+,t).$$

Thus, we obtain the total flux as

$$F(U_1(0^-,t),\cdots,U_m(0^-,t),U_{m+1}(0^+,t)) = \min\{\sum_{i=1}^{m} D_i(0^-,t), S_{m+1}(0^+,t)\}.$$

The proportions, α_i, can be determined by so-called "distribution schemes", which distribute the total flux to each upstream link. In (Newell, 1993), an on-ramp is given total priority and can send its maximum flow. In (Daganzo, 1995), a priority-based scheme was proposed. In (Lebacque, 1996), a general scheme was proposed, and it was suggested to distribute out-fluxes according to the number of lanes of upstream links. In (Banks, 2000), an on-ramp is given total priority, but its flow is also restricted by the metering rate. In (Jin and Zhang, 2003), a fair scheme is proposed to distribute out-fluxes according to local traffic demands of upstream links. In (Ni and Leonard, 2005), a fair share of the downstream supply is assigned to each upstream proportional to its capacity, and out-fluxes are then determined by comparing the corresponding fair shares and demands. With these distribution schemes, the entropy condition, (13), yields unique solutions of boundary fluxes with given interior states.

2.3   Summary of the solution framework

To solve the Riemann problem with the initial conditions in (6)-(7), we will first find stationary and interior states that satisfy the aforementioned entropy condition, admissible conditions, and traffic conservation equations. Then the kinematic wave on each link will be determined by the Riemann problem of the corresponding LWR model with initial and stationary states as initial conditions (Jin et al., 2009). Here we will only focus on solving the stationary states on all links. We can see that the feasible domains of stationary and interior states are independent of the upstream supply,

S_i, and the downstream demand, D_{m+1}. That is, the same upstream demand and downstream supply will yield the same solutions of stationary and interior states. However, the upstream and downstream wave types and speeds on each can be related to S_i as shown in Figure 4(d) and D_{m+1} as shown in Figure 5(d).

3   Solutions of two merge models

In this paper, we solve the Riemann problem for a merging junctions with two upstream links; i.e., $m = 2$. Different merge models have different entropy conditions (13). In this section, we consider two entropy conditions, i.e., two merge models. Here we attempt to find the relationships between the boundary fluxes and the initial conditions.

$$q_i = \hat{F}_i(U_1, U_2, U_3). \tag{15}$$

In contrast to local, discrete flux functions $F_i(U_1(0^-,t), U_2(0^-,t), U_3(0^+,t))$, $\hat{F}_i(U_1, U_2, U_3)$ can be considered as global, continuous. With the global, continuous fluxes, we can find stationary states from Corollary 2.2. With the solution framework in the preceding section, we can then find the kinematic waves of the Riemann problem with initial conditions (U_1, U_2, U_3).

3.1   A fair merge model

We consider the fair merging rule proposed in (Jin and Zhang, 2003), in which

$$\alpha_i = \frac{D_i(0^-,t)}{D_1(0^-,t) + D_2(0^-,t)}, \quad i = 1, 2. \tag{16}$$

Obviously, the optimization problem of (13) subject to the fair merging rule yields the following solutions

$$q_i = \min\{1, \frac{S_3(0^+,t)}{D_1(0^-,t) + D_2(0^-,t)}\} D_i(0^-,t), \quad i = 1, 2. \tag{17}$$

Thus in the Riemann solutions, stationary and interior states have to satisfy (17), traffic conservation, and the corresponding admissible conditions.

Theorem 3.1 *For the Riemann problem with the initial conditions in (6) and (7), stationary and interior states satisfying the entropy condition in (17), traffic conservation equations, and the corresponding admissible conditions are the following:*

1. *When $D_1 + D_2 < S_3$, $U_i^- = U_i(0^-,t) = (D_i, C_i)$ $(i = 1,2)$ and $U_3^+ = U_3(0^+,t) = (D_1 + D_2, C_3)$;*

2. *When $D_1 + D_2 = S_3$, $U_i^- = U_i(0^-,t) = (D_i, C_i)$ $(i = 1,2)$, $U_3^+ = (C_3, S_3)$, $U_3(0^+,t) = (C_3, S_3)$ or $(D_3(0^+,t), S_3(0^+,t))$ with $D_3(0^+,t) \geq S_3$ and $S_3(0^+,t) > S_3$ when $S_3 < C_3$;*

3. *When $D_i > \frac{C_i}{C_1+C_2}S_3$ $(i = 1,2)$, $U_3^+ = U_3(0^+,t) = (C_3, S_3)$, and $U_i^- = U_i(0^-,t) = (C_i, \frac{C_i}{C_1+C_2}S_3)$.*

4. *When $D_1 + D_2 > S_3$ and $D_i \leq \frac{C_i}{C_1+C_2}S_3$ $(i, j = 1$ or 2 and $i \neq j)$, $U_3^+ = U_3(0^+,t) = (C_3, S_3)$, $U_i^- = (D_i, C_i)$, $U_i(0^-,t) = (\frac{C_j}{S_3-D_i}D_i, C_i)$, and $U_j^- = U_j(0^-,t) = (C_j, S_3 - D_i)$.*

The proof of the theorem is given in Appendix A. In Figure 8, we demonstrate how to obtain the pair of (D_1, D_2) from initial states U_1 and U_2 and how to obtain the line of $S_3 - S_3$ in the supply-demand diagrams. According to the relationship between (D_1, D_2) and S_3, the domain of (D_1, D_2) can be divided into four regions. In Figure 9, we further demonstrate how to obtain stationary states for all these four regions. The results are consistent with those in (Daganzo, 1996) in principle: for initial conditions in region I, there are no queues on upstream links; for initial states in region II, there is a queue on link 2; for initial states in region III, there are queues on both links; and, for initial states in region IV, there is a queue on link 1.

Corollary 3.2 *For the Riemann problem with initial conditions in (6) and (7), the boundary fluxes satisfying the entropy condition in (17), traffic conservation equations, and the corresponding admissible conditions are in the following:*
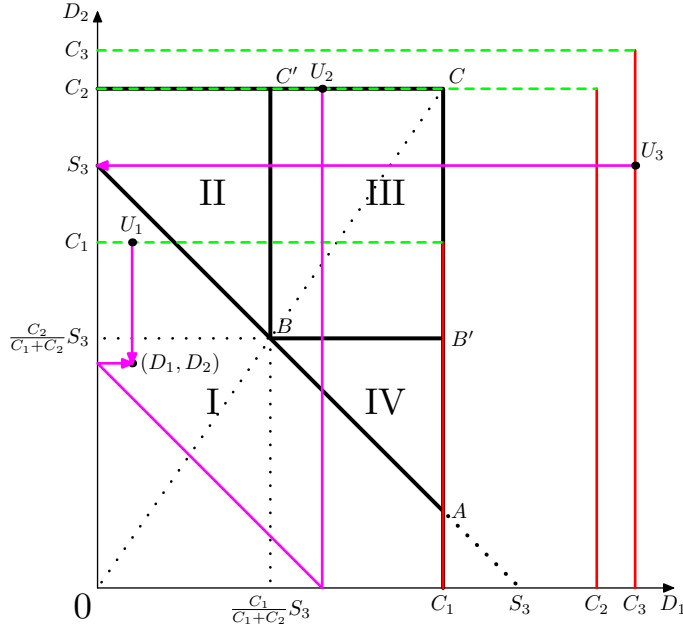
Figure 8: Four types of solutions for a fair merge model

1. *When $D_1 + D_2 \leq S_3$, $q_i = D_i$ ($i = 1, 2$) and $q_3 = D_1 + D_2$;*

2. *When $D_i > \frac{C_i}{C_1 + C_2} S_3$ ($i = 1, 2$), $q_i = \frac{C_i}{C_1 + C_2} S_3$ and $q_3 = S_3$;*

3. *When $D_1 + D_2 > S_3$ and $D_i \leq \frac{C_i}{C_1 + C_2} S_3$ ($i, j = 1$ or 2 and $i \neq j$), $q_i = D_i$, $q_j = S_3 - D_i$, and $q_3 = S_3$.*

That is, for $i, j = 1$ or 2 and $i \neq j$,

$$q_i \quad = \quad \min\{D_i, \max\{S_3 - D_j, \frac{S_3}{C_1 + C_2} C_i\}\}. \tag{18}$$

The solutions of fluxes in four different regions are shown in Figure 10, in which the dots represent the initial conditions in (D_1, D_2), and the end points of the arrows represent the solutions of fluxes (q_1, q_2). The fluxes in (18) are exactly the same as in (Ni and Leonard, 2005). In this sense, the discrete merge model with (17) converges to the merge model in (Ni and Leonard, 2005).
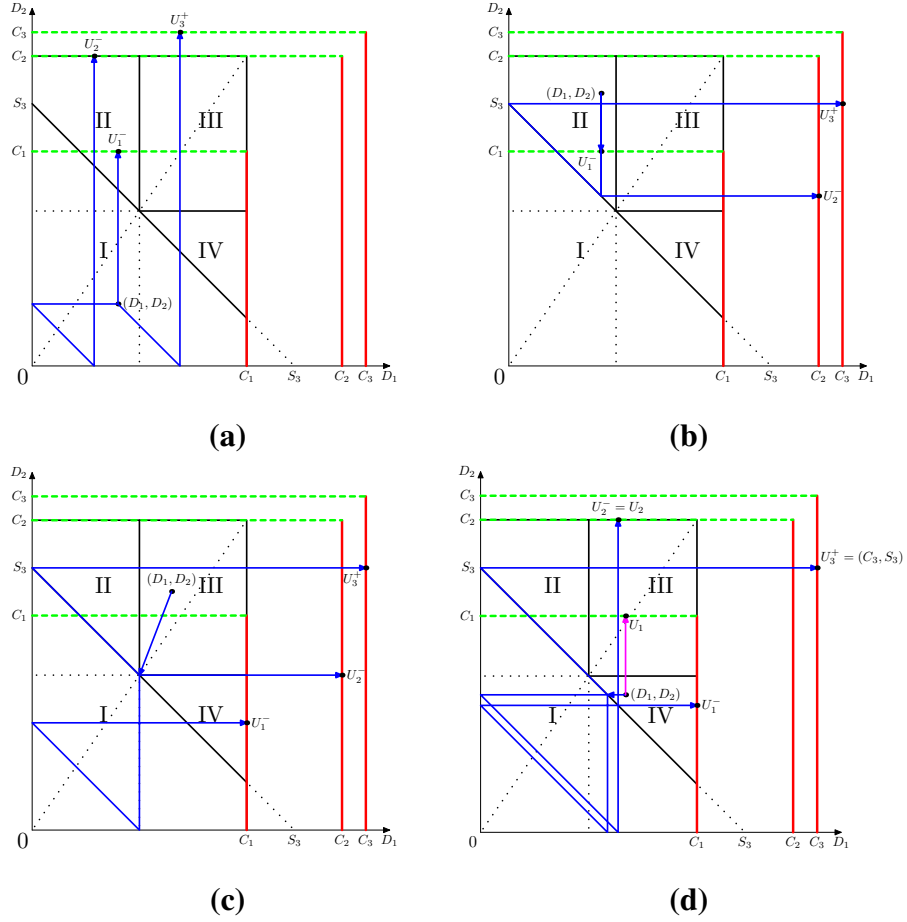
18

Figure 9: Solutions of stationary states for different initial conditions for the fair merge model

Corollary 3.3 *If U_i ($i = 1,2$) and U_3 satisfy*

$$
\begin{aligned}
\min\{D_i, S_i\} &= \min\{D_i, \max\{S_3 - D_j, \frac{S_3}{C_1 + C_2}C_i\}\}, \\
\min\{D_3, S_3\} &= \min\{D_1, \max\{S_3 - D_2, \frac{S_3}{C_1 + C_2}C_1\}\} + \min\{D_2, \max\{S_3 - D_1, \frac{S_3}{C_1 + C_2}C_2\}\} \\
&= \min\{D_1 + D_2, S_3\},
\end{aligned}
$$

then the unique stationary states are the same as the initial states, and traffic dynamics at the merging junction are stationary.
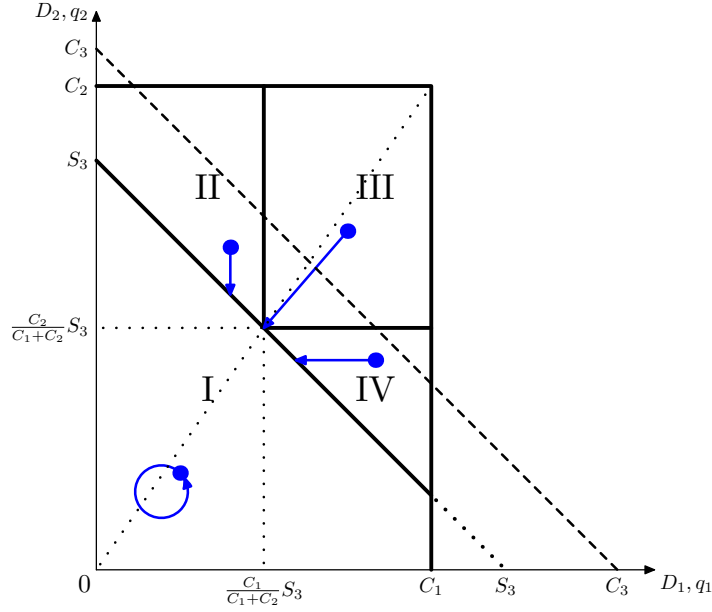
Figure 10: Solutions of fluxes for the fair merge model

Proof. The results follow from Theorem 3.1, from which we can see that stationary states U_i^- and S_3^+ satisfy

$$
\min\{D_i^-, S_i^-\} = \min\{D_i^-, \max\{S_3^+ - D_j^-, \frac{S_3^+}{C_1 + C_2} C_i\}\},
$$

$$
\min\{D_3^+, S_3^+\} = \min\{D_1^-, \max\{S_3^+ - D_2^-, \frac{S_3^+}{C_1 + C_2} C_1\}\} + \min\{D_2^-, \max\{S_3^+ - D_1^-, \frac{S_3^+}{C_1 + C_2} C_2\}\}
$$

$$
= \min\{D_1^- + D_2^-, S_3^+\}.
$$

∎

3.2   A constant merge model

We consider a merge model proposed in (Lebacque, 1996), in which

$$
q_i = \min\{D_i(0^-, t), \alpha_i S_3(0^+, t)\}, \quad i = 1, 2 \tag{19}
$$

where α_i are constant distribution proportions, $\alpha_i \in [0, 1]$, and $\sum_i \alpha_i = 1$.

20

Theorem 3.4 *For the Riemann problem with the initial conditions in (6) and (7), boundary fluxes satisfying the entropy condition in (19), traffic conservation equations, and the corresponding admissible conditions are the following:*

1. *When $D_1 + D_2 < S_3$ and $D_i \leq \alpha_i C_3$ ($i = 1, 2$), $q_i = D_i$ and $q_3 = D_1 + D_2$;*

2. *When $D_i > \alpha_i C_3$ and $D_j < S_3 - \alpha_i C_3$ ($i, j = 1$ or 2 and $i \neq j$), $q_i = \alpha_i C_3$, $q_j = D_j$, and $q_3 = \alpha_i C_3 + D_j$.*

3. *When $D_1 + D_2 \geq S_3$, $S_3 - \alpha_j C_3 \leq D_i \leq \alpha_i S_3$ ($i, j = 1$ or 2 and $i \neq j$), $q_i = D_i$, $q_j = S_3 - D_i$, and $q_3 = S_3$.*

4. *When $D_i \geq \alpha_i S_3$ ($i = 1, 2$), $q_i = \alpha_i S_3$, and $q_3 = S_3$.*

That is, for $i, j = 1$ or 2 and $i \neq j$,

$$q_i = \min\{D_i, \alpha_i C_3, \max\{S_3 - D_j, \alpha_i S_3\}\}. \tag{20}$$

The proof of the theorem is in Appendix B. The solutions of fluxes in six different regions are shown in Figure 11, in which the starting point of an arrow represents initial conditions, (D_1, D_2), and the ending point represents the solution of fluxes, (q_1, q_2). With the fluxes, we can easily find all stationary and interior states as in Theorem 3.1. Compared with the fair merging rule, the constant merging rule yield sub-optimal solutions in regions II and VI in Figure 11, in which $q_3 < \min\{D_1 + D_2, S_3\}$. That is, this merge model does not satisfy the optimization entropy condition in (14).

4   Invariant merge models

For the two merge models in the preceding section, the local, discrete flux functions $F_i(\cdot, \cdot, \cdot)$ are not the same as the global, continuous flux functions $\hat{F}_i(\cdot, \cdot, \cdot)$. That is, boundary fluxes computed
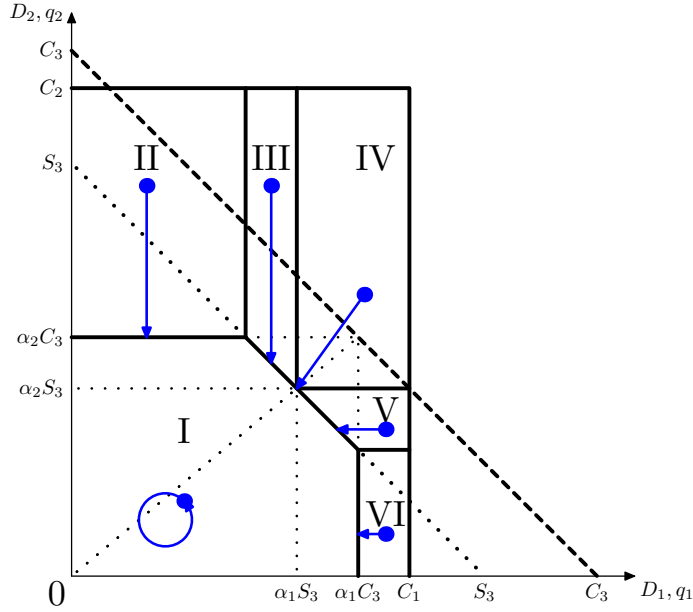
21

Figure 11: Solutions of fluxes for the constant merge model

from local flux functions are not constant. In this sense, the fair and constant merge models are not invariant. In the following, we propose two invariant merge models, in which $F_i(\cdot,\cdot,\cdot)$ and $\hat{F}_i(\cdot,\cdot,\cdot)$ have the same functional form.

4.1 An optimal invariant merge model

We consider the following priority-based merge model (Daganzo, 1995, 1996), in which $i,j = 1$, or 2 and $i \neq j$

$$q_i = \min\{D_i(0^-,t), \max\{S_3(0^+,t) - D_j(0^-,t), \alpha_i S_3(0^+,t)\}\}, \tag{21}$$

where α_i are priority distribution proportions, $\alpha_i \in [0,1]$, and $\sum_i \alpha_i = 1$.

Theorem 4.1 *For the Riemann problem with the initial conditions in (6) and (7), boundary fluxes satisfying the entropy condition in (21), the traffic conservation equations, and the corresponding*

22

admissible conditions are the following:

$$q_i = \min\{D_i, \max\{S_3 - D_j, \alpha_i S_3\}\}, \quad i, j = 1, \text{ or } 2, \text{ and } i \neq j \tag{22}$$

The proof of the theorem is given in Appendix C. Since $F_i(\cdot, \cdot, \cdot) = \hat{F}_i(\cdot, \cdot, \cdot)$, the merge model (21) is invariant. From the proof, we can see that the merging rule is optimal in the sense that $q_3 = \min\{D_1 + D_2, S_3\}$. The solutions of fluxes in four different regions are shown in Figure 12, in which the starting point of an arrow represents the initial demands, (D_1, D_2), and the end point represents the solutions of fluxes, (q_1, q_2). Note that, when $\alpha_i = \frac{C_i}{C_1 + C_2}$ $(i = 1, 2)$, then the distribution scheme is the same as (18). Therefore, the merge model in (Ni and Leonard, 2005) is invariant.
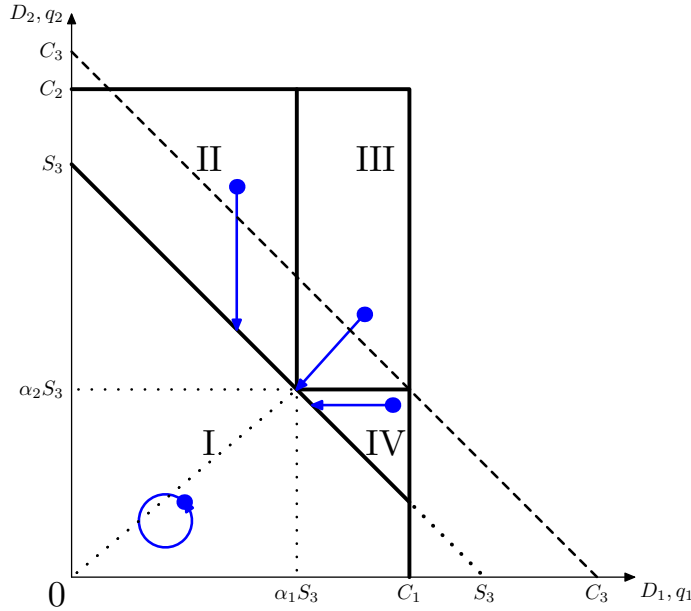

Figure 12: Solutions of fluxes for the priority-based merge model

When $\alpha_i > \frac{C_i}{C_1 + C_2}$, the merge model (21) gives higher priority to vehicles from upstream link i. Thus, (21) is another representation of the priority merge model proposed in (Daganzo, 1995, 1996). For an extreme merge model with $\alpha_1 = 1$ and $\alpha_2 = 0$ (Newell, 1993; Banks, 2000), vehicles

from link 1 is given absolute priorities. In this case, we have

$$q_1 = \min\{D_1, S_3\},$$

$$q_2 = \min\{D_2, \max\{S_3 - D_1, 0\}\}.$$

4.2 A suboptimal invariant merge model

Similarly, the continuous version of the constant merge model will lead to another invariant merge model, in which

$$q_i = \min\{D_i(0^-,t), \alpha_i C_3, \max\{S_3(0^+,t) - D_j(0^-,t), \alpha_i S_3(0^+,t)\}\}, \quad i,j = 1, \text{ or } 2, \text{ and } i \neq j \quad (23)$$

with $\alpha_i \in [0,1]$, and $\sum_i \alpha_i = 1$.

Theorem 4.2 *For the Riemann problem with initial conditions in (6) and (7), the boundary fluxes satisfying the entropy condition in (21), traffic conservation equations, and the corresponding admissible conditions are in the following:*

$$q_i = \min\{D_i, \alpha_i C_3, \max\{S_3 - D_j, \alpha_i S_3\}\}, \quad i,j = 1, \text{ or } 2, \text{ and } i \neq j \quad (24)$$

The proof of the theorem is omitted. The merge model (23) is obviously invariant. In addition, the solutions of fluxes in six different regions are the same as in Figure 11. We can see that this merge model is suboptimal. Assuming that both links 1 and 3 are the mainline freeway with capacity $C_1 = C_3$ and $D_1 = S_3 = C_1$, and link 2 is a metered on-ramp with a metering rate $D_2 \leq C_2 < C_1$. When $D_1 > \alpha_1 C_3$, and the metering rate $D_2 < \alpha_2 C_3$, then $q_1 = \alpha_1 C_3$ and $q_2 = D_2$. In this case, $q_3 = \alpha_1 C_3 + D_2$, and the utilization rate of link 3's capacity is

$$\frac{q_3}{\min\{D_1 + D_2, C_3\}} = \frac{\alpha_1 C_3 + D_2}{\min\{D_1 + D_2, C_3\}} = \frac{\alpha_1 C_3 + D_2}{C_3} \geq \alpha_1.$$

That is, as much as α_2 of link 3's capacity is wasted. In contrast, if we increase the metering rate of link 2, such that $D_2 \geq \alpha_2 C_3$. Then (23) predicts $q_3 = C_3$. That is, low metering rates could cause a lower utilization rate of link 3's capacity. This property of the merge model (23) is counter-intuitive, and the merge model is not physical.

5 Numerical examples

In this section, we numerically solve various merge models and demonstrate the validity of our analytical results. Here, both links 1 and 3 are two-lane mainline freeways with a corresponding normalized maximum sensitivity fundamental diagram (Del Castillo and Benitez, 1995) is ($\rho \in [0,2]$)

$$Q(\rho) = \rho \left\{ 1 - \exp \left[1 - \exp \left(\frac{1}{4} (\frac{2}{\rho} - 1) \right) \right] \right\}.$$

Link 2 is a one-lane on-ramp with a fundamental diagram as ($\rho \in [0,1]$)

$$Q(\rho) = \frac{1}{2} \rho \left\{ 1 - \exp \left[1 - \exp \left(\frac{1}{4} (\frac{1}{\rho} - 1) \right) \right] \right\}.$$

Note that here the free flow speed on the on-ramp is half of that on the mainline freeway, which is 1. Thus we have the capacities $C_1 = C_3 = 4C_2 = 0.3365$ and the corresponding critical densities $\rho_{c1} = \rho_{c3} = 2\rho_{c2} = 0.4876$. The length of all three links is the same as $L = 10$, and the simulation time is $T = 360$.

In the following numerical examples, we discretize each link into M cells and divide the simulation time interval T into N steps. The time step $\Delta t = T/N$ and the cell size $\Delta x = L/M$, with $\Delta t = 0.9\Delta x$, satisfy the CFL condition (Courant et al., 1928)

$$v_f \frac{\Delta t}{\Delta x} = \frac{\Delta t}{\Delta x} = 0.9 \leq 1.$$

Then we use the following finite difference equation for link $i = 1, 2, 3$:

$$\rho_{i,m}^{n+1} = \rho_{i,m}^n + \frac{\Delta t}{\Delta x} (q_{i,m-1/2}^n - q_{i,m+1/2}^n),$$

where $\rho_{i,m}^n$ is the average density in cell m of link i at time step n, and the boundary fluxes $q_{i,m-1/2}^n$ are determined by supply-demand methods. For example, for upstream links $i = 1$ and 2, the in-fluxes are

$$q_{i,m-1/2}^n = \min\{D_{i,m-1}^n, S_{i,m}^n\}, \quad m = 1, \cdots, M,$$

25

where $D_{i,m-1}^n$ is the demand of cell $m-1$ on link i, $S_{i,m}^n$ the supply of cell m, and $D_{i,0}^n$ the demand of link i. For link 3, the out-fluxes are

$$q_{3,m+1/2}^n = \min\{D_{3,m}^n, S_{3,m+1}^n\}, \quad m = 1, \cdots, M,$$

where $S_{3,M+1}^n$ is the supply of the destination. Then the out-fluxes of the upstream links and the in-flux of the downstream link are determined by merge models, which are discrete versions of (13):

$$q_{i,M+1/2}^n = F_i(D_{1,M}^n, D_{2,M}^n, S_{3,1}^n),$$
$$q_{3,1/2}^n = q_{1,M+1/2}^n + q_{2,M+1/2}^n.$$

In our numerical studies, we only consider the fair merge model (17) and its invariant counterpart (21). That is, in the fair merge model, we have

$$q_{i,M+1/2}^n = \min\{D_{i,M}^n, \frac{D_{i,M}^n}{D_{1,M}^n + D_{2,M}^n} S_{3,1}^n\},$$
$$q_{3,1/2}^n = \min\{D_{1,M}^n + D_{2,M}^n, S_{3,1}^n\}.$$

In the invariant fair merge model, we have ($i, j = 1, 2$ and $i \neq j$)

$$q_{i,M+1/2}^n = \min\{D_{i,M}^n, \max\{S_{3,1}^n - D_{j,M}^n, \alpha_i S_{3,1}^n\}\},$$
$$q_{3,1/2}^n = \min\{D_{1,M}^n + D_{2,M}^n, S_{3,1}^n\},$$

where $\alpha_i = C_i/(C_1 + C_2)$.

5.1 Kinematic waves, stationary states, and interior states in the fair merge model

In this subsection, we study numerical solutions of the fair merge model in (17). Initially, links 1 and 3 carry UC flows with $\rho_1 = \rho_3 = 0.35$, and at $t = 0$ a traffic stream on link 2 starts to merge

into link 3 with $\rho_2 = 0.1$. That is, the initial conditions in supply-demand space is $U_1 = U_3 = (0.3131, 0.3365)$ and $U_2 = (0.0500, 0.0841)$. Here we use the Neumann boundary condition in supply and demand (Colella and Puckett, 2004): $D^n_{1,0} = D^n_{1,1}$, $D^n_{2,0} = D^n_{2,1}$, and $S^n_{3,M+1} = S^n_{3,M}$. Therefore, we have a Riemann problem here.

In this case, $D_1 + D_2 = 0.3631 > S_3 = 0.3365$ and $D_2 \le \frac{C_2}{C_1+C_2} S_3 = 0.0673$. Thus according to Theorem 3.1, we have the following stationary and interior states $U_3^+ = U_3(0^+, t) = (C_3, S_3) = (C_1, C_1)$, $U_2^- = (D_2, C_2)$, $U_2(0^-, t) = (\frac{C_1}{S_3 - D_2} D_2, C_2)$, and $U_1^- = U_1(0^-, t) = (C_1, S_3 - D_2)$. Furthermore, from the LWR model, there will be a back-traveling shock wave on link 1 connecting U_1 to U_1^-, no wave on link 2, and a rarefaction wave on link 3 connecting U_3^+ to U_3.
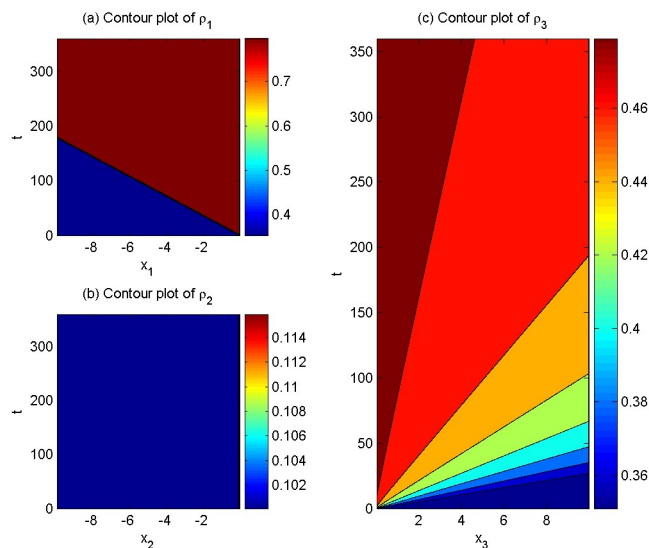

Figure 13: Solutions of the fair merge model (17): $M = 160, N = 6400$.

In Figure 13, the solutions of ρ_1, ρ_2, and ρ_3 are demonstrated with $M = 160$ and $N = 6400$. From the figures, we can clearly observe the predicted kinematic waves. In Figure 13(b) there is a very thin layer of higher densities in the last cell of the upstream link near the merging junction, which is caused by the interior state as predicted. In addition, we can observe at $t = T$ the approximate asymptotic values: $U_1^- = U_1(0^-, t) = (0.3365, 0.2865)$, and $\rho_1^- = \rho_1(0^-, t) =$

0.8277; $U_2^- = (0.05, 0.0841)$, $U_2(0^-, t) = (0.0587, 0.0841)$, $\rho_2^- = 0.1$, $\rho_2(0^-, t) = 0.1179$; $U_3^+ = (0.3365, 0.3365)$, and $\rho_3^+ = \rho_{c3} = 0.4874$. These numbers are all very close to the theoretical values and get closer if we reduce Δx or increase T. That is, the results are consistent with theoretical results asymptotically.
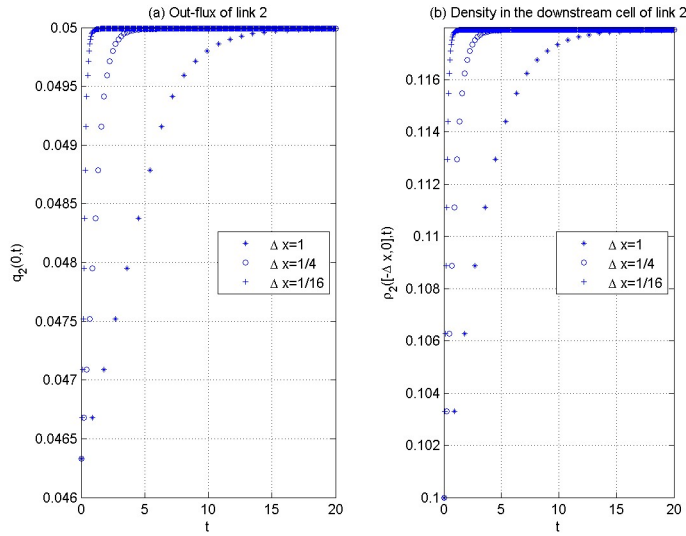

Figure 14: Evolution of the out-flux and the density in the downstream cell of link 2 for the fair merge model (17)

In Figure 14, we demonstrate the evolution of the out-flux and the density in the downstream cell of link 2 for three different cell sizes. From Figure 14(a) we can see that, initially, the out-flux of link 2 is

$$\frac{D_2}{D_1 + D_2} S_3 = \frac{0.05}{0.05 + 0.3131} 0.3365 = 0.0463,$$

which is not the same but approaches the asymptotic out-flux $D_2 = 0.05$. Correspondingly the density in the downstream cell of link 2 approaches the interior state, as shown in Figure 14(b). Furthermore, as we decrease the cell size, the numerical results are closer to the theoretical ones at the same time instant. This figure shows that the fair merge model is not invariant, but approaches

its invariant counterpart asymptotically. Note that the densities in any other cells of link 2 remain constant at 0.1.

5.2   Comparison of non-invariant and invariant merge models

In this subsection, we compare the numerical solutions of the fair merge model (17) with its invariant counterpart (22). Initially, links 1 and 3 carry UC flows with $\rho_1 = \rho_3 = 0.35$, and at $t = 0$ a traffic stream on link 2 starts to merge into link 3 with $\rho_2 = 0.1$. Different from the example in the preceding subsection, here we use the following boundary conditions: $D_{1,0}^n = D_{1,1}^n$, $D_{2,0}^n = 0.05 + 0.03\sin(n\pi\Delta t/60)$, and $S_{3,M+1}^n = S_{3,M}^n$. Thus we have a periodic demand on link 2.

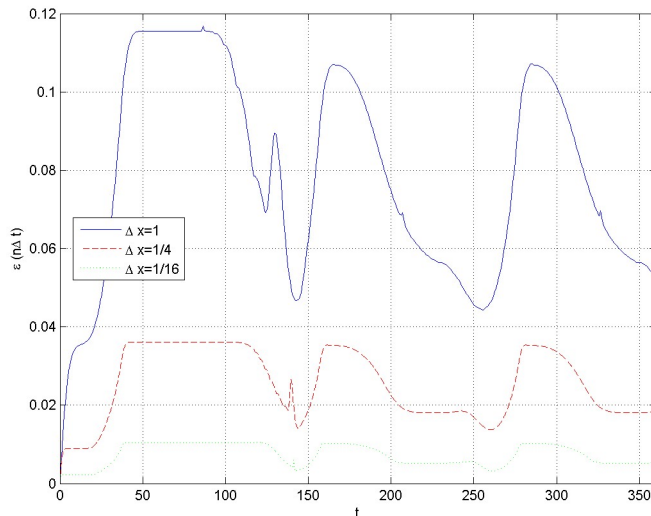Figure 15: Difference in the solutions between the fair merge model (17) and its invariant counterpart (21)

We use $\rho_{i,m}^n$ for the discrete density from the fair merge model (17) and $\bar{\rho}_{i,m}^n$ from its invariant counterpart (22). Then we denote the difference between the two solutions by

$$\varepsilon(n\Delta t) \;=\; \sum_{i=1}^{3}\sum_{m=1}^{M} |\rho_{i,m}^n - \bar{\rho}_{i,m}^n|\Delta x. \tag{25}$$

In Figure 15, we can see that the difference decreases if we decreases the cell size. This clearly demonstrates that the fair merge model (17) converges to its invariant counterpart (21).

6 Conclusion

In this paper, we studied continuous kinematic wave models of merging traffic flow which are consistent with discrete CTM with various distribution schemes. In particular, we introduced the supply-demand diagram of traffic flow and proposed a solution framework for the Riemann problem of merging traffic flow. In the Riemann solutions, each link can have two new states, an interior state and a stationary state, and the kinematic waves on a link are determined by the initial state and the stationary state. We then derived admissible conditions for interior and stationary states and introduced various distribution schemes as entropy conditions defined in the interior states. Then we proved that stationary states and boundary fluxes exist and are unique for the Riemann problem for both the fair and constant distribution schemes. We also discussed two invariant merge models, in which the local and discrete flux is the same as the global and continuous flux. With numerical examples, we demonstrated the validity of the proposed analytical framework and that the fair merge model converges to its invariant counterpart when we decrease the cell size. Compared with existing discrete kinematic wave models (i.e. CTM with various distribution schemes) of merging traffic flow, the continuous models can provide analytical insights on kinematic waves arising at merging junctions; and, compared with existing analytical models, they are physically meaningful and consistent with existing CTM.

In this study, we introduced a new definition of invariant merge models, in which fluxes computed by discrete models should be the same as those by their continuous counterparts. An important observation is that both the fair and constant merge models are not invariant. For example, for the fair merge model, at $t = 0$ the local fluxes from (17) are

$$q_i = \min\{1, \frac{S_3}{D_1 + D_2}\}D_i, \quad i = 1, 2,$$

30

which are different from (18) when only one upstream is congested; i.e., when $D_1 + D_2 > S_3$ and $D_i \leq \frac{C_i}{C_1+C_2}S_3$. However, the results here suggest that the discrete fluxes converge to the continuous ones after a sufficient amount of time or at a given time but with decreasing time intervals. That is, the non-invariant discrete merge models do not provide incorrect solutions but just approximate solutions to the corresponding continuous merge models. Compared with invariant discrete merge models, the fair merging model has some unique merits; e.g., it can be easily extended to general junctions with multiple upstream links as shown in (Jin and Zhang, 2003, 2004). Note that, as demonstrated in (Jin et al., 2009), invariant models can also yield interior states.

This paper presents a systematic framework for solving kinematic waves arising from merging traffic in supply-demand space. We expect that boundary fluxes, stationary states, and kinematic waves for other distribution schemes can also be solved in this framework. For example, we can obtain the stationary states and kinematic waves for the following artificial merge model

$$q_i = \min\{1, \frac{0.9S_3(0^+,t)}{D_1(0^-,t)+D_2(0^-,t)}\}D_i(0^-,t), \quad i = 1, 2,$$

in which only 90% of the downstream supply can be utilized by the upstream traffic.

The Riemann problem for a merge with three or more upstream links can be discussed in the same framework, but, due to the space limitations, this will be discussed in future studies. Generally, there are systematic lane-changing activities at merging junctions, and existing merge models based on supply-demand method cannot capture the impacts of lane-changes (Laval et al., 2005). In the future, it would be interesting to analyze the formation and dissipation of traffic queues at merging junctions when lane-changes are considered.

Acknowledgements

for improving the presentation of the paper. The views and results contained herein are the author's alone.

References

Ansorge, R., 1990. What does the entropy condition mean in traffic flow theory? Transportation Research Part B 24 (2), 133–143.

Banks, J., 2000. Are minimization of delay and minimization of freeway congestion compatible ramp metering objectives? Transportation Research Record: Journal of the Transportation Research Board 1727, 112–119.

Bar-Gera, H., Ahn, S., 2009. Empirical macroscopic evaluation of freeway merge-ratios. Transportation Research Part C In Press.

Bultelle, M., Grassin, M., Serre, D., 1998. Unstable Godunov discrete profiles for steady shock waves. SIAM Journal on Numerical Analysis 35 (6), 2272–2297.

Cassidy, M., Ahn, S., 2005. Driver turn-taking behavior in congested freeway merges. Transportation Research Record: Journal of the Transportation Research Board 1934, 140–147.

Coclite, G., Garavello, M., Piccoli, B., 2005. Traffic flow on a road network. SIAM Journal on Mathematical Analysis 36, 1862.

Colella, P., Puckett, E. G., 2004. Modern Numerical Methods for Fluid Flow. In draft.

Courant, R., Friedrichs, K., Lewy, H., 1928.
"Uber die partiellen Differenzengleichungen der mathematischen Physik. Mathematische Annalen 100, 32–74.

Daganzo, C. F., 1994. The cell transmission model: a dynamic representation of highway traffic consistent with hydrodynamic theory. Transportation Research Part B 28 (4), 269–287.

Daganzo, C. F., 1995. The cell transmission model II: Network traffic. Transportation Research Part B 29 (2), 79–93.

Daganzo, C. F., 1996. The nature of freeway gridlock and how to prevent it. Proceedings of the 13th International Symposium on Transportation and Traffic Theory, 629–646.

Del Castillo, J. M., Benitez, F. G., 1995. On the functional form of the speed-density relationship - II: Empirical investigation. Transportation Research Part B 29 (5), 391–406.

Engquist, B., Osher, S., 1980. Stable and entropy satisfying approximations for transonic flow calculations. Mathematics of Computation 34 (149), 45–75.

Hidas, P., 2002. Modelling lane changing and merging in microscopic traffic simulation. Transportation Research Part C 10 (5-6), 351–371.

Hidas, P., 2005. Modelling vehicle interactions in microscopic simulation of merging and weaving. Transportation Research Part C 13 (1), 37–62.

Holden, H., Risebro, N. H., 1995. A mathematical model of traffic flow on a network of unidirectional roads. SIAM Journal on Mathematical Analysis 26 (4), 999–1017.

Jin, W., 2009. Asymptotic traffic dynamics arising in diverge–merge networks with two intermediate links. Transportation Research Part B 43 (5), 575–595.

Jin, W.-L., Chen, L., Puckett, E. G., 2009. Supply-demand diagrams and a new framework for analyzing the inhomogeneous Lighthill-Whitham-Richards model. Proceedings of the 18th International Symposium on Transportation and Traffic Theory, 603–635.

Jin, W.-L., Zhang, H. M., 2003. On the distribution schemes for determining flows through a merge. Transportation Research Part B 37 (6), 521–540.

Jin, W.-L., Zhang, H. M., 2004. A multicommodity kinematic wave simulation model of network traffic flow. Transportation Research Record: Journal of the Transportation Research Board 1883, 59–67.

Laval, J., Cassidy, M., Daganzo, C., 2005. Impacts of lane changes at merge bottlenecks: a theory and strategies to maximize capacity. Presented at the Traffic and Granular Flow Conference, Berlin, Germany.

Lebacque, J., Khoshyaran, M., 2005. First order macroscopic traffic flow models: Intersection modeling, Network modeling. Proceedings of the 16th International Symposium on Transportation and Traffic Theory, 365–386.

Lebacque, J. P., 1996. The Godunov scheme and what it means for first order traffic flow models. Proceedings of the 13th International Symposium on Transportation and Traffic Theory, 647–678.

Lighthill, M. J., Whitham, G. B., 1955. On kinematic waves: II. A theory of traffic flow on long crowded roads. Proceedings of the Royal Society of London A 229 (1178), 317–345.

Newell, G. F., 1993. A simplified theory of kinematic waves in highway traffic I: General theory. II: Queuing at freeway bottlenecks. III: Multi-destination flows. Transportation Research Part B 27 (4), 281–313.

Ni, D., Leonard, J., 2005. A simplified kinematic wave model at a merge bottleneck. Applied Mathematical Modelling 29 (11), 1054–1072.

Nie, Y., Zhang, H., 2008. Oscillatory Traffic Flow Patterns Induced by Queue Spillback in a Simple Road Network. Transportation Science 42 (2), 236.

Papageorgiou, M., 1990. Dynamic modelling, assignment and route guidance in traffic networks. Transportation Research Part B 24 (6), 471–495.

Papageorgiou, M., Kotsialos, A., 2002. Freeway ramp metering: An overview. IEEE Transactions on Intelligent Transportation Systems 3 (4), 271–281.

Peeta, S., Ziliaskopoulos, A., 2001. Foundations of Dynamic Traffic Assignment: The Past, the Present and the Future. Networks and Spatial Economics 1 (3), 233–265.

Richards, P. I., 1956. Shock waves on the highway. Operations Research 4 (1), 42–51.

van Leer, B., 1984. On the relation between the upwind-differencing schemes of Godunov, Engquist-Osher and Roe. SIAM Journal on Scientific and Statistical Computing 5 (1), 1–20.

Appendix A: Proof of Theorem 3.1

Proof. From traffic conservation equations in (8) and admissible conditions of stationary states, we can see that

$$q_3 \leq \min\{D_1 + D_2, S_3\}.$$

We first demonstrate that it is not possible that $q_3 < \min\{D_1 + D_2, S_3\} \leq \min\{C_1 + C_2, C_3\}$. Otherwise, from (10) and (12) we have $U_3(0^+, t) = U_3^+ = (q_3, C_3)$ with $q_3 < S_3$; Since $q(U_1^-) + q(U_2^-) = q_3 < D_1 + D_2$, then we have $q(U_i^-) < D_i$ for at least one upstream link, e.g., $q_1 < D_1$. From (9) and (11) we have $U_1(0^-, t) = U_1^- = (C_1, q_1)$. Then from the entropy condition in (17) we have

$$
\begin{aligned}
q_3 &= \min\{C_1 + D_2(0^-, t), C_3\}, \\
q_1 &= \min\{1, \frac{C_3}{C_1 + D_2(0^-, t)}\}C_1.
\end{aligned}
$$

Since $q_3 < C_3$, from the first equation we have $q_3 = C_1 + D_2(0^-, t) < C_3$, and from the second equation we have $q_1 = C_1$, which contradicts $q_1 < D_1$. Therefore,

$$q_1 + q_2 = q_3 = \min\{D_1 + D_2, S_3\}.$$

That is, the fair distribution scheme yields the optimal fluxes for any initial conditions.

(1) When $D_1 + D_2 < S_3$, we have $q_3 = D_1 + D_2 < S_3$. From (10) and (12) we have $U_3(0^+, t) = U_3^+ = (D_1 + D_2, C_3)$. Since $q_1 + q_2 = D_1 + D_2$ and $q_i \leq D_i$, we have $q_i = D_i$. From (9) we have $U_i^- = (D_i, C_i)$. From (11) we have $U_i(0^-, t) = (D_i(0^-, t), S_i(0^-, t))$ with $S_i(0^-, t) \geq D_i^- = D_i$. From (17) we have

$$
\begin{aligned}
q_3 &= \min\{D_1(0^-, t) + D_2(0^-, t), C_3\} = D_1 + D_2 < S_3 \leq C_3, \\
q_i &= \min\{1, \frac{C_3}{D_1(0^-, t) + D_2(0^-, t)}\}D_i(0^-, t) = D_i.
\end{aligned}
$$

Thus, $D_i(0^-, t) = D_i \leq S_i(0^-, t)$. Then $U_i(0^-, t) = U_i^- = (D_i, C_i)$. In this case, there are no interior states on all links.

(2) When $D_1 + D_2 = S_3$, we have $q_3 = S_3$. From (10) and (12), we have $U_3^+ = (C_3, S_3)$ and $U_3(0^+, t) = (D_3(0^+, t), S_3(0^+, t))$ with $D_3(0^+, t) \geq S_3^+ = S_3$. Since $q_1 + q_2 = D_1 + D_2$ and $q_i \leq D_i$, we have $q_i = D_i$. From (9) and (11), we have $U_i^- = (D_i, C_i)$ and $U_i(0^-, t) = (D_i(0^-, t), S_i(0^-, t))$ with $S_i(0^-, t) \geq D_i^- = D_i$. From (17) we have

$$
\begin{aligned}
q_3 &= \min\{D_1(0^-, t) + D_2(0^-, t), S_3(0^+, t)\} = D_1 + D_2 = S_3, \\
q_i &= \min\{1, \frac{S_3(0^+, t)}{D_1(0^-, t) + D_2(0^-, t)}\} D_i(0^-, t) = D_i.
\end{aligned}
$$

We can have the following two scenarios.

(i) If $D_1(0^-, t) + D_2(0^-, t) \geq S_3(0^+, t) = D_1 + D_2 = S_3 \leq D_3(0^+, t)$, then $U_3(0^+, t) = U_3^+ = (C_3, S_3)$ and there is no interior state on link 3. Moreover, we have

$$
\frac{D_1 + D_2}{D_1(0^-, t) + D_2(0^-, t)} D_i(0^-, t) = D_i,
$$

which leads to $D_i(0^-, t) \leq D_i \leq S_i(0^-, t)$. From the assumption that $D_1(0^-, t) + D_2(0^-, t) \geq D_1 + D_2$, we have $D_i(0^-, t) = D_i$. Further we have $U_i(0^-, t) = U_i^- = (D_i, C_i)$, and there are no interior states on links 1 or 2.

(ii) If $S_3(0^+, t) > D_1(0^-, t) + D_2(0^-, t) = D_1 + D_2 = S_3$, $D_i(0^-, t) = D_i$. Thus $U_i(0^-, t) = U_i^- = (D_i, C_i)$, and there are no interior states on links 1 or 2. Moreover, $U_3(0^+, t)$ satisfies $S_3(0^+, t) > S_3$ and $D_3(0^+, t) \geq S_3$. Thus there can be multiple interior states on link 3 when $S_3 < C_3$.

(3,4) When $D_1 + D_2 > S_3$, for upstream links, at least one of the stationary states is SOC. Otherwise, from (9) we have $U_i^- = (D_i, C_i)$, and $q_1 + q_2 = D_1 + D_2 > S_3$, which is impossible. In addition, we have $q_3 = S_3 < D_1 + D_2$. From (10) we have $U_3^+ = (C_3, S_3)$. From (12) we have $U_3(0^+, t) = (D_3(0^+, t), S_3(0^+, t))$ with $D_3(0^+, t) \geq S_3^+ = S_3$. From (17) we have

$$
\begin{aligned}
q_3 &= \min\{D_1(0^-, t) + D_2(0^-, t), S_3(0^+, t)\} = S_3 < D_1 + D_2, \\
q_i &= \min\{1, \frac{S_3(0^+, t)}{D_1(0^-, t) + D_2(0^-, t)}\} D_i(0^-, t).
\end{aligned}
$$

37

If $D_1(0^-,t) + D_2(0^-,t) \leq S_3(0^+,t)$, then $D_1(0^-,t) + D_2(0^-,t) = S_3 < D_1 + D_2$ and $q_i = D_i(0^-,t)$. This is not possible for the SOC stationary state $U_i^- = U_i(0^-,t) = (C_i,q_i)$ with $q_i < D_i \leq C_i$. Thus $S_3(0^+,t) < D_1(0^-,t) + D_2(0^-,t)$, $S_3(0^+,t) = S_3 < D_1 + D_2$, and $U_3(0^+,t) = U_3^+ = (C_3,S_3)$. Hence for both upstream links

$$q_i \;=\; \frac{S_3}{D_1(0^-,t) + D_2(0^-,t)} D_i(0^-,t).$$

(3) When $D_i > \frac{C_i}{C_1+C_2} S_3$ ($i = 1,2$), stationary states on both links 1 and 2 are SOC with $U_i^- = U_i(0^-,t) = (C_i,q_i)$ with $q_i < D_i$. Otherwise, we assume that link 1 is SOC with $U_1(0^-,t) = U_1^- = (C_1,q_1)$ and link 2 is UC with $U_2^- = (D_2,C_2)$. Then

$$D_2 \;=\; \frac{S_3}{C_1 + D_2(0^-,t)} D_2(0^-,t) \leq \frac{S_3}{C_1+C_2} C_2 < D_2,$$

which is impossible. From (17), we have

$$q_i = \frac{S_3}{C_1+C_2} C_i,$$

and $U_i(0^-,t) = U_i^- = (C_i,q_i)$.

(4) When $D_1 + D_2 > S_3$ and $D_i \leq \frac{C_i}{C_1+C_2} S_3$ ($i,j = 1$ or 2 and $i \neq j$), we can show that stationary states on links j and i are SOC and UC respectively with $U_j^- = U_j(0^-,t) = (C_j,q_j)$ with $q_j < D_j$, $U_i^- = (D_i,C_i)$, and $S_i(0^-,t) \geq D_i$. Otherwise, $U_i(0^-,t) = U_i^- = (C_i,q_i)$ with $q_i < D_i$, and

$$q_i \;=\; \frac{S_3}{C_i + D_j(0^-,t)} C_i \geq \frac{C_i}{C_1+C_2} S_3 \geq D_i,$$

which is impossible. Since at least one of the upstream links has SOC stationary state, the stationary states on links i and j are UC and SOC respectively. From (17), we have a unique interior state on link i, $U_i(0^-,t) = (\frac{D_i}{S_3-D_i} C_j, C_i)$, and $q_j = S_3 - D_i$.

For the four cases, it is straightforward to show that (18) always holds. ∎

Appendix B: Proof of Theorem 3.4

Proof.

(1) When $D_1 + D_2 < S_3$ and $D_i \leq \alpha_i C_3$ $(i = 1, 2)$, then $q_3 < S_3$, and $U_3^+ = U_3(0^+, t) = (q_3, C_3)$. Assuming that $q_i < D_i \leq C_i$, then $U_i^- = U_i(0^-, t) = (C_i, q_i)$. From (19), we have $q_i = \min\{C_i, \alpha_i C_3\} = \alpha_i C_3 < D_i$, which contradicts $D_i \leq \alpha_i C_3$. Therefore, $q_i = D_i$ and $q_3 = D_1 + D_2$.

(2) When $D_i > \alpha_i C_3$ and $D_j < S_3 - \alpha_i C_3$ $(i, j = 1$ or 2 and $i \neq j)$, we first prove that $q_i < D_i$ and then $q_j = D_j$.

    (i) If $q_i = D_i$, then from (19), we have $\alpha_i C_3 < D_i = \min\{D_i(0^-, t), \alpha_i S_3(0^+, t)\} \leq \alpha_i S_3(0^+, t)$, which leads to $C_3 < S_3(0^+, t)$. This contradicts $C_3 \geq S_3(0^+, t)$. Thus, $q_i < D_i$, and $U_i^- = U_i(0^-, t) = (C_i, q_i)$.

    (ii) If $q_j < D_j \leq C_j$, then $U_j^- = U_j(0^-, t) = (C_j, q_j)$. From (19), we have $q_j = \min\{C_j, \alpha_j S_3(0^+, t)\} = \alpha_j S_3(0^+, t) < D_j < S_3 - \alpha_i C_3 \leq \alpha_j C_3$. Thus $S_3(0^+, t) < C_3$. Since $q_i = \alpha_i S_3(0^+, t)$, we have $q_3 = q_i + q_j < \alpha_i S_3(0^+, t) + S_3 - \alpha_i C_3 < S_3$, which leads to $U_3^+ = U_3(0^+, t) = (q_3, C_3)$. This contradicts $S_3(0^+, t) < C_3$. Therefore, $q_j = D_j$.

From (19), we have $q_i = \alpha_i S_3(0^+, t)$. Thus $q_3 = q_i + q_j < S_3 - \alpha_i C_3 + \alpha_i S_3(0^+, t) \leq S_3$. Then, $U_3^+ = U_3(0^+, t) = (q_3, C_3)$, $q_i = \alpha_i C_3$, $q_3 = \alpha_i C_3 + D_j$.

(3) When $D_1 + D_2 \geq S_3$, $S_3 - \alpha_j C_3 \leq D_i \leq \alpha_i S_3$ $(i, j = 1$ or 2 and $i \neq j)$, we first prove that $q_3 = S_3$ and then that $q_i = D_i$. Therefore $q_i = D_i$, and $q_j = S_3 - D_i$.

    (i) If $q_3 < S_3$, then $U_3^+ = U_3(0^+, t) = (q_3, C_3)$. We first prove that at least one upstream stationary state is SOC and then that none of the upstream stationary states can be SOC. Therefore, $q_3 = S_3$.

39

(a) If none of the upstream stationary states are SOC, then $q_i = D_i$ $(i = 1, 2)$, and $q_3 = q_1 + q_2 = D_1 + D_2 \geq S_3$, which contradicts $q_3 < S_3$.

(b) Assuming that $q_i < D_i$, then $U_i^- = U_i(0^-, t) = (C_i, q_i)$. From (19), we have $q_i = \min\{C_i, \alpha_i C_3\} = \alpha_i C_3 < D_i$. This is not possible, since $D_i \leq \alpha_i S_3$. Thus, $q_i = D_i$.

(c) Assuming that $q_j < D_j$, then $U_j^- = U_j(0^-, t) = (C_j, q_j)$. From (19), we have $q_j = \min\{C_j, \alpha_j C_3\} = \alpha_j C_3$. Then $D_i = q_i = q_3 - \alpha_j C_3 < S_3 - \alpha_j C_3$, which contradicts $D_i \geq S_3 - \alpha_j C_3$.

(ii) Now assume $q_i < D_i$, then $U_i^- = U_i(0^-, t) = (C_i, q_i)$. From (19), we have $q_i = \min\{C_i, \alpha_i S_3(0^+, t)\} = \alpha_i S_3(0^+, t) < D_i \leq \alpha_i S_3$. Therefore, $q_j \leq \alpha_j S_3(0^+, t) < \alpha_j S_3$, which leads to $q_i + q_j < S_3$. This is not possible, since $q_i + q_j = S_3$.

(4) When $D_i \geq \alpha_i S_3$, we first prove that $q_3 = S_3$ and then that $q_i \geq \alpha_i S_3$ $(i = 1, 2)$. Therefore, $q_i = \alpha_i S_3$ $(i = 1, 2)$, and $q_3 = S_3$.

(i) If $q_3 < S_3$, then $U_3^+ = U_3(0^+, t) = (q_3, C_3)$. We first prove that at least one upstream stationary state is SOC and then that none of the upstream stationary states can be SOC. Therefore $q_1 + q_2 = q_3 = S_3$.

(a) If none of the upstream stationary states are SOC, then $q_i = D_i$ $(i = 1, 2)$, and $q_3 = D_1 + D_2 \geq S_3$, which contradicts $q_3 < S_3$.

(b) Assuming that $q_i < D_i$, then $U_i^- = U_i(0^-, t) = (C_i, q_i)$. From (19), we have $q_i = \min\{C_i, \alpha_i C_3\} = \alpha_i C_3$. Then $q_j = q_3 - q_i < S_3 - \alpha_i C_3 \leq \alpha_j S_3 \leq D_j$. Thus, $U_j^- = U_j(0^-, t) = (C_j, q_j)$, and from (19) we have $q_j = \min\{C_j, \alpha_j C_3\} = \alpha_j C_3 > \alpha_j S_3$, which contradicts $q_j < \alpha_j S_3$. Thus, U_i^- is UC and $q_i = D_i$.

(c) Similarly we can prove that U_j^- is UC and $q_j = D_j$.

(ii) If $q_i < \alpha_i S_3 \leq D_i \leq C_i$, then $U_i^- = U_i(0^-, t) = (C_i, q_i)$. From (19), we have $q_i = \min\{C_i, \alpha_i S_3(0^+, t)\} = \alpha_i S_3(0^+, t) < \alpha_i S_3$. Therefore, $q_j \leq \alpha_j S_3(0^+, t) < \alpha_j S_3$, which

40

leads to $q_i + q_j < S_3$. This is not possible, since $q_i + q_j = S_3$.

For the four cases, it is straightforward to show that (20) always holds. ∎

Appendix C: Proof of Theorem 4.1

Proof.

First (21) implies that

$$q_3 = \min\{D_1(0^-,t) + D_2(0^-,t), S_3(0^+,t)\},$$

which can be shown for three cases: (i) $D_1(0^-,t) + D_2(0^-,t) < S_3(0^+,t)$, (ii) $D_i(0^-,t) \geq \alpha_i S_3(0^+,t)$, and (iii) $D_1(0^-,t) + D_2(0^-,t) \geq S_3(0^+,t)$ and $D_i(0^-,t) \leq \alpha_i S_3(0^+,t)$.

(1) When $D_1 + D_2 < S_3$, $q_3 = q_1 + q_2 \leq D_1 + D_2 < S_3 \leq C_3$. Thus the downstream stationary state is SUC with $U_3^+ = U_3(0^+,t) = (q_3, C_3)$. In the following, we prove that $q_i = D_i$, which is consistent with (22). Therefore (22) is correct in this case.

    (i) Assuming that $q_i < D_i \leq C_i$, then the stationary state on link i is SOC with $U_i^- = U_i(0^-,t) = (C_i, q_i)$. From (21), we have

$$q_i = \min\{C_i, \max\{C_3 - D_j(0^-,t), \alpha_i C_3\}\} = \max\{C_3 - D_j(0^-,t), \alpha_i C_3\} < C_i,$$
$$q_j = \min\{D_j(0^-,t), \max\{C_3 - C_i, \alpha_j C_3\}\}.$$

    We show that the two equations have no solutions for either $\alpha_j C_3 \leq D_j(0^-,t)$ or $\alpha_j C_3 > D_j(0^-,t)$. Thus $q_i = D_i$.

        (a) When $\alpha_j C_3 \leq D_j(0^-,t)$, we have $\alpha_i C_3 \geq C_3 - D_j(0^-,t)$. From the first equation we have $q_i = \alpha_i C_3$. From the second equation we have $q_j = D_j(0^-,t) \geq \alpha_j C_3$ or $q_j = \max\{C_3 - C_i, \alpha_j C_3\} \geq \alpha_j C_3$. Thus $q_i + q_j \geq C_3 \geq S_3$, which contradicts $q_3 < S_3$.

41

(b) When $\alpha_j C_3 > D_j(0^-,t)$, we have $\alpha_i C_3 < C_3 - D_j(0^-,t)$. From the first equation we have $q_i = C_3 - D_j(0^-,t)$. From the second equation we have $q_j = D_j(0^-,t)$. Thus $q_i + q_j = C_3$, which contradicts $q_3 < S_3$.

(2) When $D_i \geq \alpha_i S_3$, $S_3 - D_j \leq \alpha_i S_3$. In the following we show that $q_3 = S_3$ and $q_i = \alpha_i S_3$, which is consistent with (22).

(i) If $q_3 < S_3$, then the stationary state on link 3 is SUC with $U_3^+ = U_3(0^+,t) = (q_3, C_3)$. Also at least one of the upstream stationary states is SOC, since, otherwise, $q_1 + q_2 = D_1 + D_2 \geq S_3$. Here we assume $U_i^- = U_i(0^-,t) = (C_i, q_i)$. From (21) we have

$$q_i = \min\{C_i, \max\{C_3 - D_j(0^-,t), \alpha_i C_3\}\} = \max\{C_3 - D_j(0^-,t), \alpha_i C_3\},$$

$$q_j = \min\{D_j(0^-,t), \max\{C_3 - C_i, \alpha_j C_3\}\}.$$

We show that the two equations have no solutions for either $C_3 - D_j(0^-,t) \geq \alpha_i C_3$ or $C_3 - D_j(0^-,t) < \alpha_i C_3$. Thus $q_3 = S_3$.

(a) If $C_3 - D_j(0^-,t) \geq \alpha_i C_3$, $D_j(0^-,t) \leq \alpha_j C_3$. From the first equation we have $q_i = C_3 - D_j(0^-,t)$. From the second equation we have $q_j = D_j(0^-,t)$. Thus $q_i + q_j = C_3$, which contradicts $q_3 < S_3 \leq C_3$.

(b) If $C_3 - D_j(0^-,t) < \alpha_i C_3$, $D_j(0^-,t) > \alpha_j C_3$. From the first equation we have $q_i = \alpha_i C_3$. From the second equation we have $q_j = D_j(0^-,t) > \alpha_j C_3$ or $q_j = \max\{C_3 - C_i, \alpha_j C_3\} \geq \alpha_j C_3$. Thus $q_i + q_j \geq C_3$, which contradicts $q_3 < S_3 \leq C_3$.

(ii) If $q_i < \alpha_i S_3 \leq D_i \leq C_i$ for any $i = 1, 2$, then $U_i^- = U_i(0^-,t) = (C_i, q_i)$. From (21) we have

$$q_i = \max\{S_3(0^+,t) - D_j(0^-,t), \alpha_i S_3(0^+,t)\} < C_i,$$

$$q_j = \min\{D_j(0^-,t), \max\{S_3(0^+,t) - C_i, \alpha_j S_3(0^+,t)\}\}.$$

The first equation implies that $\alpha_i S_3(0^+,t) < \alpha_i S_3$; i.e., $S_3(0^+,t) < S_3$. In addition, $S_3(0^+,t) - D_j(0^-,t) < \alpha_i S_3$. Thus, $S_3(0^+,t) - C_i < S_3 - C_i < S_3 - \alpha_i S_3 = \alpha_j S_3$, and

$\max\{S_3(0^+,t)-C_i,\alpha_j S_3(0^+,t)\} < \alpha_j S_3$. From the second equation we have $q_j < \alpha_j S_3$. Thus $q_i+q_j < S_3$, which contradicts $q_i+q_j = S_3$. Thus $q_i \geq \alpha_i S_3$ for $i = 1,2$. Since $q_i+q_j = S_3$, $q_i = \alpha_i S_3$.

(3) When $D_i+D_j \geq S_3$ and $D_i \leq \alpha_i S_3$ for $i,j = 1$ or 2 and $i \neq j$. In the following we show that $q_3 = S_3$ and $q_i = D_i$, which is consistent with (22).

   (i) If $q_3 < S_3$, then the stationary state on link 3 is SUC with $U_3^+ = U_3(0^+,t) = (q_3,C_3)$. We first prove that at least one upstream stationary state is SOC and then that none of the upstream stationary states can be SOC. Therefore, $q_3 = S_3$.

     (a) If none of the upstream stationary states are SOC, then $q_1+q_2 = D_1+D_2 \geq S_3$, which contradicts $q_3 < S_3$. Thus, at least one of the upstream stationary states is SOC.

     (b) Assuming that $q_i < D_i$, then $U_i^- = U_i(0^-,t) = (C_i,q_i)$. From (21) we have

$$q_i \;=\; \min\{C_i, \max\{C_3-D_j(0^-,t),\alpha_i C_3\}\} = \max\{C_3-D_j(0^-,t),\alpha_i C_3\} < D_i,$$

     which is not possible, since $D_i \leq \alpha_i S_3$. Thus $q_i = D_i$.

     (c) Assuming that $q_j < D_j$, then $U_j^- = U_j(0^-,t) = (C_j,q_j)$. Since $q_3 = \min\{D_i(0^-,t)+ C_j,C_3\} < S_3$, we have $q_3 = D_i(0^-,t)+C_j < S_3$. From (21) we have $D_i = q_i \leq D_i(0^-,t)$. Thus $D_i+D_j \leq D_i(0^-,t)+C_j < S_3$, which contradicts $D_i+D_j \geq S_3$.

  (ii) If $q_i < D_i$, then $U_i^- = U_i(0^-,t) = (C_i,q_i)$. From (21), we have

$$q_i \;=\; \max\{S_3(0^+,t)-D_j(0^-,t),\alpha_i S_3(0^+,t)\} < D_i \leq \alpha_i S_3,$$
$$q_j \;=\; \min\{D_j(0^-,t),\max\{S_3(0^+,t)-C_i,\alpha_j S_3(0^+,t)\}\}.$$

From the first equation we have that $S_3(0^+,t) < S_3$. We show that the two equations have no solutions for either $S_3(0^+,t) - D_j(0^-,t) \geq \alpha_i S_3(0^+,t)$ or $S_3(0^+,t) - D_j(0^-,t) < \alpha_i S_3(0^+,t)$. Therefore $q_i = D_i$.

43

(a) When $S_3(0^+,t) - D_j(0^-,t) \geq \alpha_i S_3(0^+,t)$, we have $D_j(0^-,t) \leq \alpha_j S_3(0^+,t)$. Thus $q_i = S_3(0^+,t) - D_j(0^-,t)$ and $q_j = D_j(0^-,t)$. Then $q_i + q_j = S_3(0^+,t) < S_3$, which contradicts $q_i + q_j = S_3$.

(b) When $S_3(0^+,t) - D_j(0^-,t) < \alpha_i S_3(0^+,t)$, we have $q_i = \alpha_i S_3(0^+,t)$ and $S_3(0^+,t) - C_i < S_3(0^+,t) - q_i = \alpha_j S_3(0^+,t)$. Thus $q_j \leq \alpha_j S_3(0^+,t)$, and $q_i + q_j \leq S_3(0^+,t) < S_3$, which contradicts $q_3 = S_3$.

∎